TRPV3 channel activity helps cortical neurons stay active during fever.

Yiming Shen[1], Richárd Fiáth[2], István Ulbert[2,3,4], Michelle W. Antoine[1,5]*

[1]*Section on Neural Circuits, National Institute of Alcohol Abuse and Alcoholism, National Institutes of Health, Bethesda, MD 20892, USA.*

[2]*Institute of Cognitive Neuroscience and Psychology, Research Centre for Natural Sciences, Eötvös Loránd Research Network, Budapest, Hungary; Faculty of Information Technology and Bionics, Pázmány Péter Catholic University, Budapest, Hungary.*

[3]*Faculty of Information Technology and Bionics, Pázmány Péter Catholic University, Budapest, Hungary*

[4]*Center of Neurosurgery and Neurointervention, Semmelweis University, Budapest, Hungary*

[5] Lead contact

*Correspondence and requests for materials should be addressed to: michelle.antoine@nih.gov (M.W.A).

Conflict of interest statement: The authors declare no competing financial interests.

Abstract

Fever raises body temperature (T_b) from ~37°C to beyond 38°C to combat pathogens. While generally well tolerated below 40°C, fevers can induce seizures in 2-5-year-old neurotypical children. This study investigates how neuronal activity is maintained during fever-range temperatures. Recordings of layer (L) 4-evoked spiking in L2/3 mouse somatosensory cortex show that excitatory pyramidal neurons (PNs) may remain inactive, stay active, cease activity, or initiate activity as temperature rises from 30°C (standard in electrophysiology studies) to 36°C (normal T_b) and then to 39°C (fever-range). Similar proportions of neurons cease or initiate spiking. Thus, "STAY" PNs, which remain active across temperatures changes, are crucial for maintaining stable spiking activity. STAY PNs are more prevalent at younger postnatal ages. To sustain spiking during temperature increases, STAY PNs adjust their depolarization levels to match the spike threshold while remaining temperature-insensitive in input resistance. In the striatum, STAY medium-spiny neurons are likely dopamine (D)2-type receptor-expressing and share similar characteristics with STAY PNs. Intracellular blockade of the thermosensitive channel *TRPV3*, but not *TRPV4*, significantly decreased the population of STAY PNs and reduced spiking at 39°C. Therefore, *TRPV3* function may be critical for maintaining cortical activity during fever.

Keywords: development; TRPV3 channel; TRPV4 channel; fever; temperature; seizures; network stability.

Introduction

In most mammals, including humans, core body temperature (T_b) is tightly regulated between 36.1 and 37.8°C, with a daily fluctuation of 0.5°C (Campbell I, 2008). Fever or thermal challenges can impede heat dissipation to significantly increase T_b beyond 38°C (Wang et al., 2014). Since global brain and T_b are largely congruent, these large temperature elevations affect both areas (Wang et al., 2014). T_b increases up to 40°C are generally well-tolerated, but temperatures above 42°C are noxious, causing protein breakdown and cell death. The body and brain have protective mechanisms, such as heat shock proteins, to handle heat stress. These proteins are rapidly induced or upregulated at noxious temperatures to aid in refolding and degrading damaged proteins upon return to physiological temperatures (Miller and Fort, 2018). However, mechanisms that preserve firing activity at lower, more physiological temperatures within the fever-range are not well understood.

In rare cases, moderate-grade fevers (Tb = 38.1 to 39°C) cause seizures in children aged 6 months to 6 years, with the highest susceptibility between 2 and 5 years (Oakley et al., 2009, Shinnar and O'Dell, 2004). These febrile seizures (FS) are almost typically triggered by the thermal aspect of fever, as infections or metabolic disorders are absent (Shinnar and O'Dell, 2004). Additionally, FS can be induced solely by increased T_b due to ambient heat, such as a warm bath, hot room, or overdressing. FS generally do not occur beyond five years of age, suggesting the development of biophysiological properties that stabilize brain activity during fever within this 2- to 5-year-old window of susceptibility (Shinnar and O'Dell, 2004). In rodents, there is also an age-dependent susceptibility to seizures induced via exposure to innocuous temperatures (37.5-40°C), which rapidly decreases and is quickly abolished within the first 1-2 postnatal weeks (Holtzman et al., 1981). Seizures induced by noxious heat above 42.5°C likely

arise via different mechanisms, as such temperatures are associated with cellular protein breakdown and death.

For practical reasons, EEG recordings for the onset of FS in humans are limited. However, EEG traces from rodents with thermally induced seizures show that ictal events often initiate in the hippocampus and propagate to the cortex, with the later spread to the cortex being correlated to the more severe behavioral stages of the seizure i.e. Racine stage > 4 (Dube et al., 2010; Baram et al., 1997). Thus, the cortex represents a critical locus in the seizure phenotype and likely contains mechanisms that may alter neural activity in response to temperature changes. Using wildtype mice across three postnatal developmental periods—postnatal day (P)7-8 (neonatal/early), P12-14 (infancy/mid), and P20-26 (juvenile/late)—we investigated the electrophysiological properties, *ex vivo* and *in vivo*, that enable excitatory pyramidal neurons (PNs) neurons in mouse primary somatosensory (S1) cortex to remain active during temperature increases from 30°C (standard in electrophysiology studies) to 36°C (physiological temperature), and then to 39°C (fever-range).

We also attempted to generalize our findings by performing similar recordings of evoked activity in two main striatal projection cell types: medium spiny neurons (MSNs) expressing dopamine (D)1-type receptors ($D1^+$ MSNs) and D2-type receptors ($D2^+$ MSNs). As very few studies have recorded activity in striatal neurons at fever temperatures, these studies also help inform about functional effects of fever temperature on striatal cell function. Furthermore, in humans and mice, methamphetamine (a misused substance), which targets the striatum, can significantly elevate T_b, as much as 3.5–4.0°C above basal levels (Brown et al., 2003), so these studies may help uncover neuronal cell types that function at these elevated temperatures to exert behavioral effects.

Lastly, to begin to identify molecular determinants that may mediate the electrophysiological properties that enable PNs to remain spiking, we extended our studies to two members of a family of thermosensitive, Ca^{2+}-permeable, nonselective cation channels, the transient receptor potential vanilloid 3-4 (*TRPV* 3-4) channels, that are activated within the innocuous warm temperature range (31-39°C) (Su et al., 2023; Shibasaki et al., 2007). Other members, like *TRPV1* and *TRPV2* are activated by noxious heat above 42°C and 52°C (Kasho and Tominaga, 2022). *TRPV3* and *TRPV4* share low (~41%) amino acid sequence overlap (Smith et al., 2002) and differ somewhat in the temperature threshold for activation. *TRPV3* and *TRPV4* are both expressed in the brain (Xu et al., 2002; Caterina MJ, 2007; Kanju et al., 2016; Chen et al., 2022) and are activated between 31–39°C and >27-34 °C, respectively (Su et al., 2023; Shibasaki et al., 2007).

In this study, we aimed to elucidate the adaptative neural mechanisms that enable excitatory PNs to maintain spiking despite substantial increases in brain temperature into the fever range. Our electrophysiological assessments were conducted across three postnatal stages, during which susceptibility to fever-induced seizures naturally varied. With temperature increases from 30°C to 39°C, excitatory PNs responded to depolarizing stimuli by either remaining inactive, staying spiking, ceasing spiking, or initiating spiking. Nearly equal proportions of neurons ceased or initiated activity, so firing stability was largely maintained by the PNs that remained active throughout temperature increases, i.e., the STAY neurons. STAY neurons likely sustain spiking across temperatures due to their unique ion channel composition, including *TRPV3*, which allows for higher depolarization levels through increased excitatory synaptic input relative to inhibitory input.

Results

Body Temperature rises to fever levels during regular activity and exposure to higher ambient temperatures.

Contrary to common belief, T_b is not fixed but varies with arousal state, motor activity, and environmental temperature (Kiyatkin EA, 2019; Hankenson et al., 2018**;** Wang et al., 2014). Using a sterile IPTT-300 implantable temperature transponder (Bio Medic Data Systems, LLC) with a 0.025-second time constant and 0.1°C accuracy, T_b measurements were recorded every five-minutes over six hours from 2–3-week-old wildtype mice in an open-field arena at room temperature (Figure 1A). This analysis revealed a stable median temperature of 36.5°C with a maximum and minimum fluctuation of 0.5°C (Figure 1A). However, within-subject analysis showed brief T_b elevations into the fever range (shaded red bars) during increased activity like cage climbing or digging (Figure 1B-C). Exposure to infrared light elevates ambient temperatures and induces prolonged T_b elevations into the fever range, with an onset within minutes and a duration of several hours (Fig.1D).

Spiking in P12-P14 cortical excitatory pyramidal neurons remains stable as temperature enters the fever range.

To investigate how postnatal cortical neurons respond to fever-range temperature, we used whole-cell current clamp electrophysiology to record natural spiking, evoked synaptically, as brain slice temperature gradually rose from 30°C to 36°C to 39°C in PNs (Figure 2A-B). Acute S1 cortex slices (350 µm thick) were prepared using standard methods (Antoine et al., 2019). PNs were visually identified via infrared DIC optics, and physiological verification for regular spiking was done in current clamp. Neuronal activity in PNs was evoked by stimulating in the

barrel center of cortical layer (L) 4 using a bipolar electrode (0.2 ms pulses) at a specific stimulation intensity: 1.4X Eθ (Figure 2A). Eθ is defined as the minimal intensity evoking an excitatory postsynaptic current (EPSC) during more than 3 of 5 consecutive sweeps with 10 s inter-sweep interval. Eθ was determined in voltage clamp for each recorded cell, prior to recording post-synaptic potentials (PSPs) and spiking in current clamp. L4- evoked PSPs and spiking, were recorded from L2/3 PNs, with resting membrane potential (V_m) set just below spike threshold (-50mV) to simulate in vivo conditions (Yamashita et al., 2013).

Recordings of synaptically-evoked activity in L2/3 wildtype cortical excitatory PNs from P12-14 mice showed significant effects of temperature elevations from 30°C to 39°C. These changes resulted in an increased depolarization required to reach spike threshold (ST) (defined as the minimal V_m that just elicits spiking) (Figure 2B-C). Consistent with previous findings, measurements of input resistance (R_{in}) which reflect the extent to which membrane channels are open, showed significant reductions across all recorded neurons with increasing temperature (Figure 2D). Similar temperature-induced effects on R_{in} have been reported in L2/3 PNs in the rat visual cortex (Hardingham and Larkman, 1997) and in hippocampal CA1 and CA3 PNs from P13-P16 mice (Kim and Connors, 2012). The depolarized ST and reduced R_{in} in PNs would likely decrease cell excitability and spiking. Indeed, the percentage of spiking cells decreased during temperature elevations from 30°C to 39°C (Figure 2E). However, contrary to expectations, average spiking remained remarkably stable (Figure 2F-G).

Spiking in P7-8 cortical excitatory pyramidal neurons decreases as temperature enters the fever range.

This stability in average spiking at 39°C, despite the loss of some previously active neurons, suggests the presence of temperature-adaptive changes in PNs that help to maintain normal circuit activity levels. These changes may either initiate firing in previously non-spiking neurons

or either maintain or elevate spiking levels in currently active cells. Interestingly, in P7-8 mice, temperature elevations from 30°C to 39°C produced similar effects on ST and R_{in}, with ST increasing and R_{in} decreasing (Figure 3A-D). However, in P7-8 PNs, during temperature elevations from 36 to 39°C, ST did not increase, and R_{in} decreased (Figure 2C-D and 3C-D). Additionally, the percentage of spiking PNs decreased during temperature elevations from 30°C to 39°C (Figure 3E). In contrast to P12-14 PNs, the average spiking levels in P7-8 PNs significantly decreased during these temperature elevations (Figure 3F-G). This suggests that temperature-adaptive changes, possibly involving R_{in} and ST, which help maintain average spiking levels at fever temperatures despite the loss of some previously active neurons, may be underdeveloped or absent at this earlier age.

Increased depolarization at higher spike thresholds helps maintain stable spiking activity in cortical pyramidal neurons during temperature elevations.

The temperature-induced increases in ST at P12-14, would make it harder for a cell to spike, as larger depolarization levels would be required to maintain spiking (Figure 4A). Therefore, we hypothesized that in cells with increased ST that remain spiking, a temperature-adaptive change might involve a proportional increase in depolarization. To determine if larger depolarizations were associated with higher (less negative) STs, we analyzed the relationship between peak postsynaptic potential (PSP), which measures maximum depolarization, and ST (Figure 4B). Correlation analysis revealed a strong positive correlation between peak PSP and spike threshold at P12-14, which was absent at P7-8 and P20-23 (Figure 4C). This correlation was specific to these parameters, as it did not occur for comparisons involving input resistance, an intrinsic property which is affected by temperature changes (Figure 4D-E).

One mechanism that could promote enhanced depolarization is a reduction in the inhibitory PSP (IPSP) (Figure 4F). In addition to the early component of the PSP (the peak), where excitation is

maximal, we also quantified the late component, where inhibition levels are greatest and thus largely represents the IPSP (Bhatia et al., 2019; Antoine et al., 2019) (Figure 4B). This analysis revealed that the late PSP was significantly reduced with temperature elevations from 30°C to 39°C with (Figure 4G).Correlation analysis indicated that there was no correlation between the ST and LPSP at any age (P7-8: r=0.17, P=0.41, XY pairs=25; P12-14: r=0.24, P=0.31, XY pairs=19; P20-23: r=0.33, P=0.28, XY pairs=13 Pearson's test). However, a significant, moderate relationship occurred between the magnitude of the LPSP and the PSP threshold (Figure 4H). Thus, PNs with increased STs and larger PSPs were part of a circuit where synaptic inhibition was reduced across all or most PNs, regardless of whether STs were elevated. These results suggest that at P12-14, ST is sensitive to temperature increases and spiking is maintained by larger depolarization levels in these neurons.

Cortical neurons that remain active at febrile temperatures spike at higher rates, but the excitatory-inhibitory balance remains unchanged.

At a later age (P24-P26), we applied external heat to elevate the T_b into fever range and used *in vivo* high-density, extracellular electrophysiological recordings to capture single-unit activity in the S1 cortex of ketamine/xylazine anesthetized wildtype mice (Figure 5A). Unlike in vitro whole-cell patch-clamp recordings, extracellular recordings allow analysis only from cells that spike throughout the recording period during temperature elevations from 36°C (baseline) to fever-range. This is largely due to the inability of spike sorting algorithms to reliably track neurons that stop firing during the recording. *In vivo*, putative excitatory PNs that remained active also increased their spike rates at fever temperatures, as did putative inhibitory neurons (Figure 5B). Consistent with these *in vivo* findings, *ex vivo* recordings at a similar age (P20-23) showed that 11.1% of recorded excitatory PNs (n=27 cells) spiked at both 36°C and 39°C (Figure 5C). However, similar to the *in vivo* condition, neurons that remained spiking at 36°C and 39°C increased their spike/firing rate (Figure 5D).

As both excitatory and inhibitory PNs that stay spiking increase their firing rates (Figure 5B) and considering that some neurons within the network are inactive throughout or stop spiking, it is plausible that these events are calibrated such that despite temperature increases, the excitatory to inhibitory (E-I) balance within the circuit may remain relatively unchanged. Indeed, recordings of L4-evoked excitatory and inhibitory postsynaptic currents (respectively EPSCs and IPSCs) in wildtype L2/3 excitatory PNs in S1 cortex, where inhibition is largely mediated by the parvalbumin positive (PV) interneurons, showed that E-I balance (defined as E/E+I, the ratio of the excitatory current to the total current) remained unchanged as temperature increased from 36 to 39°C (Figure 5E). Along with the 11.1% of recorded excitatory PNs that stayed spiking during temperature increases from 36°C to 39°C, roughly equal proportions of neurons stopped spiking and started spiking (Figure 5C). Thus, neurons that maintain spiking at fever temperatures play a crucial role in determining the overall activity levels of the circuit. Additionally, we found that the proportion of PNs that remain spiking from 36°C to 39°C is higher at earlier ages (P12-14) compared to later ages (P20-23) (Figure 5F).

Excitatory pyramidal neurons that remain spiking with temperature elevations into fever range exhibit unique intrinsic properties.

As neurons that remain spiking with temperature elevations may be crucial in setting overall cortical circuit activity levels, we sought to uncover additional information about the intrinsic characteristics of cortical PNs at P12-14 that facilitate their activity at 36°C to 39°C. We refer to neurons that retained spiking at all three temperatures (30°C, 36°C, and 39°C) as STAY neurons, while those that stopped spiking upon temperature transitions from 30°C to 36°C or 36°C to 39°C are denoted as STOP neurons. Firstly, in STOP and STAY neurons, ST increased during temperature elevations from 30°C to 39°C (Figure 6A). However, in STOP PNs, the increases in ST were greater than in those neurons that continued spiking (Figure 6A).

The ST of neurons that continued spiking at 39°C was similar in magnitude to that of neurons that stopped spiking at 36°C.

There was an interaction of temperature and whether the PNs were STOP or STAY cells in the PSP (P=0.048, two-way ANOVA, mixed-effects model), with a trend toward larger PSPs in the STAY PNs (Figure 6B). STAY cells showed a strong positive correlation between PSP and ST (Figure 6C-D). At 30°C, STAY neurons had larger LPSPs (Figure 6E). However, inhibition levels in these PNs were unique in that inhibition levels significantly decreased with temperature elevations (Figure 6E). Moreover, we found a significant moderate inverse correlation between ST and LPSP in the STAY cells that remain spiking at 39°C (r=-0.57, P=0.046, XY pairs=13, Spearman). Thus, in PNs that STAY spiking, the excitation and inhibition levels are matched to facilitate greater depolarization and maintain spiking activity. Temperature-induced alterations in spike height and spike afterhyperpolarization (AHP) were not different between STAY and STOP cells, while R_{in} was largely insensitive to temperature changes in STAY PNs but not in STOP PNs (Figure 6F-H).

Medium spiny neurons (MSNs) that remain spiking with temperature elevations into fever range exhibit unique intrinsic properties.

To determine whether the effects on ST, PSP, and R_{in} were specific to STAY PNs or also extended to other cell types, we used BAC transgenic *Drd1a-tdTomato* and *Drd2-EGFP* mice (Ade et al., 2011; Gong et al., 2003) to record evoked spiking from the two main striatal projection cell types: medium spiny neurons (MSNs) expressing dopamine (D)1-type receptors ($D1^+$ MSNs) and D2-type receptors ($D2^+$ MSNs), respectively. As with the cortical PNs recordings, firing in MSNs was evoked via a fixed magnitude of stimulation (1.4X Eθ) via an electrode placed nearby in the corpus callosum (Figure 7A). Whole-cell current clamp recordings were made from $D1^+$ MSNs and $D2^+$ MSNs in the dorsolateral striatum. Although

STAY cells were not as frequent among $D1^+$ MSNs (3/17 recorded cells), we observed an increase in ST during temperature elevations from 30°C to 39°C (Figure 7B-C). Similar to the PNs, a strong interaction effect of temperature and whether the $D1^+$ MSNs were STOP or STAY cells was observed for the PSP (P=0.041, Two-way repeated measures ANOVA, mixed-effects model). The magnitude of the PSPs in STOP $D1^+$ MSNs decreased during temperature elevations from 30°C to 39°C and 36°C to 39°C, while the PSPs in STAY cells remained unchanged (STOP (mV): 30°C: 2.96 ± 0.72, 36°C: 2.57 ± 0.40, 39°C: 1.74 ± 0.33; 36°C to 39°C: P=0.003; 30°C to 39°C: P=0.045; STAY(mV): 30°C: 2.22 ± 0.30, 36°C: 2.63 ± 0.91, 39°C: 3.90 ± 1.40, Two way repeated measures ANOVA, mixed-effects model) (Figure 7D). STAY $D1^+$ MSNs exhibited no significant correlation between PSP and ST (r=0.18, P=0.70, XY pairs=7, Pearson). Similar to PNs, in STAY $D1^+$ MSNs, R_{in} was largely insensitive to temperature increases, whereas R_{in} decreased in STOP cells (Figure 7E).

STAY cells were more abundant for the $D2^+$ MSNs (7/13 recorded cells). Like the PNs and $D1^+$ MSNs, we observed an increase in ST during temperature elevations from 30°C to 39°C (Figure 7F-G). Similar to the STOP $D1^+$ MSNs, the magnitude of the PSPs in STOP $D2^+$ MSNs decreased during temperature elevations from 36°C to 39°C, while the PSPs in STAY cells remained unchanged (STOP(mV): 30°C: 1.60 ± 0.12, 36°C: 2.22 ± 0.26, 39°C: 1.66 ± 0.27 ; 36°C to 39°C: P=0.042; STAY(mV): 30°C: 3.51 ± 0.58, 36°C: 2.53 ± 0.82, 39°C: 2.290 ± 0.41, two way repeated measures ANOVA, mixed-effects model) (Figure 7H). STAY $D2^+$ MSNs exhibited no significant correlation between PSP and ST (r=-0.28, P=0.40, XY pairs=11, Pearson). Similar to PNs, in STAY $D2^+$ MSNs, R_{in} was largely insensitive to temperature increases, whereas R_{in} decreased in STOP cells (Figure 7I). Altogether, these results suggest that STAY MSNs and PN have some shared characteristics, namely the temperature sensitivity of ST and R_{in} being insensitive to temperature increases.

Temperature elevations in the fever range increase TRPV3 currents in cortical pyramidal neurons.

Next, we tried to determine whether we could identify molecular determinants that facilitate the properties of STAY cells. We focused on the transient receptor potential vanilloid 1-4 (*TRPV*1-4) channels, a family of thermosensitive, Ca^{2+}-permeable, nonselective cation channels. However, only *TRPV3* and *TRPV4* are activated within the innocuous warm temperature range (31-39°C), whereas *TRPV1* and *TRPV2* are activated by noxious heat above 42°C and 52°C, respectively (Kasho and Tominaga, 2022). *TRPV3* has a reported temperature threshold for activation between 31–39°C, with Smith et al., 2002 noting activation at 39°C. Using whole-cell voltage clamp, we recorded *TRPV3* currents at different voltages in cortical excitatory PNs with bath application of camphor (5 mM), a *TRPV3* agonist (Moqrich et al., 2005) (Figure 8A). We observed a significant increase in *TRPV3* currents at 39°C (Figure 8B-C, two-way repeated measures ANOVA, with Fisher's LCD test). We also measured the net *TRPV3* currents by comparing TRPV3 current densities recorded in the absence and presence of a forsythoside B is a natural *TRPV3* inhibitor found in the plant *Lamiophlomis rotate* with an IC 50 of 6.7 μmol/L and no obvious inhibitory effects on the other TRPV channels like *TRPV1* or *4* (Zhang et al., 2019). Consistent with Smith et al., 2002, who noted *TRPV3* activation at 39°C, we also observed a net positive*TRPV3* current at 39°C (Figure 8D-G).

Inhibiting TRPV3, but not TRPV4 channels, significantly reduced the population of STAY pyramidal neurons and spiking levels at fever temperature.

To investigate the potential role of *TRPV3* and *TRPV4* in regulating STAY PN phenotype in the S1 cortex during temperature increases from 30-39°C, we applied the following blockers: forsythoside B (50μM) or RN1734 (10μM, *TRPV4* blocker) intracellularly in our recordings of L4-evoked spiking at 1.4X Eθ in L2/3 PNs (Figure 9A). RN1734 is a highly selective antagonist for

TRPV4 with an IC 50 of 5.9 μmol/L and minimal to negligible affinity for the other TRPV channels (Vincent et al., 2009). These blockers phenocopy electrophysiological effects observed in *Trpv4* $^{-/-}$ *KO* and *Trpv3* $^{-/-}$ *KO* mice (Chen et al., 2022). For instance, *Trpv3* $^{-/-}$ *KO* mice exhibit a hyperpolarizing effect on the resting membrane potential (RMP) in striatal MSNs and L2 stellate neurons in the entorhinal cortex (Chen et al., 2022). This hyperpolarizing effect on the RMP is mediated by *TRPV3* activation, which promotes the influx of cations (Shibasaki et al., 2007; Chen et al., 2022), and is blocked by pharmacological inhibition of *TRPV3* with 50 μmol/L forsythoside B (Chen et al., 2022). Although, temperature increases alone can hyperpolarize the RMP, consistent with these prior reports, our recordings of L4-evoked spiking in L2/3 PNs of S1 cortex also showed a significant enhancement of RMP hyperpolarization at 39°C with intracellular *TRPV3* block via forsythoside B (no block (n=13 cells) vs *TRPV3* blocker (n=15 cells): 30°C: -75.1 ± 1.1 vs -77.1 ± 1.0; 36°C: -73.5 ± 1.2 vs -76.3 ± 1.1 ; 39°C: -71.3 ± 1.0 vs -74.4 ± 1.1, P=0.048; Two-way repeated measures ANOVA, with Fisher's LCD test).

Furthermore, we found that intracellular blockade of *TRPV3* caused a significant reduction in the percentage of STAY neurons (No block: 27% (37 recorded cells), *TRPV3* block: 8% (n=26 recorded cells), *TRPV4* block: 17% (n=24 recorded cells), two-tailed binomial test) (Figure 9B). Consistent with the STAY cells being largely responsible for maintaining stable average spiking during temperature elevations, spiking was reduced in PNs with intracellular *TRPV3* blockade during the temperature transitions from 30°C to 39°C (Figure 9C). *TRPV3* block did not occlude the increases in the depolarization required to reach ST (*TRPV3* blocker: 30°C: 7.15 ± 0.57, 36°C: 8.39 ± 0.26, 39°C: 10.0 ± 0.94, 30°C vs 39°C: P=0.007, One- way repeated measures ANOVA, mixed-effects model with Tukey's test). However, it did abolish the temperature induced increases in the PSP (*TRPV3* blocker: 30°C: 2.37 ± 0.36, 36°C: 2.45 ± 0.38, 39°C: 2.22 ± 0.25; No blocker: 30°C: 2.47 ± 0.32, 36°C: 2.90 ± 0.32, 39°C: 3.32 ± 0.52 , 30 vs 39°C:

P=0.030, One-way repeated measures ANOVA, mixed-effects model with Dunnett's test). Consistently, *TRPV3* block abolished the positive correlation between ST and PSP (No block: XY pairs=27, *TRPV3* blocker: XY pairs=18, Pearson's test) (Figure 9D).

Furthermore, in keeping with the correlation between the magnitude of the LPSP and the PSP threshold, we found that *TRPV3* blockade also prevented the temperature induced decreases in the LPSP (Figure 9E). Moreover, these reductions in spiking with *TRPV3* blockade were not dependent on temperature-induced decreases in R_{in}, as changes to PNs were similar in the *TRPV3* block and no-block conditions (Figure 9F). Altogether, these results suggest that either *TRPV3* expression or the functional effects of *TRPV3* (e.g., mediating Ca^{2+} or other cation (Na^{+}, K^{+}) influx), may define the subset of STAY neurons. Given this role, loss of *TRPV3* is not expected to contribute to seizure activity but rather to promote temperature-induced hypoactivity in cortical circuits. Intriguingly, *TRPV4* blockade caused a subset of PNs to initiate spiking at 39°C (Figure 9B). Thus, low *TRPV4* expression could define cells that are likely to become active at 39°C.

Discussion

In this study, we aimed to elucidate adaptive neural mechanisms that enable excitatory PNs to remain active despite substantial increases in brain temperature into the fever range. Our electrophysiological assessments across three postnatal ages, P7-8, P12-14 and P20-23 showed that excitatory PNs responded to temperature increases from 30°C to 39°C by either remaining inactive, staying active, ceasing activity, or initiating activity. Roughly equal portions of neurons ceased or initiated activity, so firing stability was largely maintained by those that remained active, i.e., STAY neurons. The overall proportion of PNs that remain spiking from 36°C to 39°C was higher in infancy compared to juvenile ages. This increased proportion at

earlier ages could potentially reflect the increased risk for febrile seizure occurrence at earlier postnatal ages.

STAY neurons likely possess a unique composition of ion channels that enable them to exhibit temperature sensitivity in spike threshold but not in input resistance, and adjust their depolarization levels to match the ST value. Our initial characterization focused on *TRPV* 3 and TRPV4, two members of a family of thermosensitive transient receptor potential vanilloid channels that are expressed in the brain and activated between 30-39°C, the temperature range of our study. Intracellular blockade of *TRPV3*, but not *TRPV4*, significantly decreased the population of STAY PNs and prevented stability in spiking activity during temperature increases into fever range.

TRPV3 is highly expressed in various tissues, including epithelial cells of the skin and oropharynx, the tongue, testis, dorsal root ganglion, trigeminal ganglion, spinal cord and brain (Moussaieff A et al., 2008 and Xu et al., 2002). It plays a crucial role in skin and hair generation as well as in the perception of pain and warmth on the skin. However, its role in the central nervous system remains to be further elucidated. In the brain, TRPV3 is expressed in several neuronal types, including cortical and striatal neurons (Xu et al., 2002; Chen et al., 2022). *TRPV3* has a reported temperature threshold for activation between 31–39°C, with Smith et al., 2002 noting activation at 39°C. Consistent with this, we observed the strongest physiological effects in cortical PNs at 39°C. At this temperature, intracellular blockade of *TRPV3* reduced average spiking levels and temperature-induced increases in the PSP. Additionally, a potential early postnatal temperature-dependent activity mechanism in PNs, where levels of excitatory and inhibitory input are adjusted to match the cell's ST, was abolished with *TRPV3* blockade. Altogether, these results suggest that TRPV3 blockade reduces net activity in sensory cortical circuits by decreasing activity in STAY cells.

Although, *TRPV3* channels are cation-nonselective, they exhibit high permeability to Ca^{2+} (Ca2+>Na^{+}≈K^{+}≈Cs^{+}) with permeability ratios (relative to Na^{+}) of 12.1, 0.9, 0.9, 0.9 (Xu et al., 2002). Opening of *TRPV3* channels activates a nonselective cationic conductance and elevates membrane depolarization, which can increase the likelihood of generating action potentials. Indeed, our observations of a loss of the temperature-induced increases in the PSP with *TRPV3* blockade are consistent with a reduction in membrane depolarization. In S1 cortical circuits at P12-14, STAY PNs appear to rely on a temperature-dependent activity mechanism, where depolarization levels (mediated by higher excitatory input and lower inhibitory input) are scaled to match the cell's ST. Thus, an inability to increase PSPs with temperature elevations prevents PNs from reaching ST, so they cease spiking.

Previous research in *Trpv3* $^{-/-}$ KO mice revealed a similar phenotype of reduced activity with diminished *TRPV3* function (Chen et al., 2022). Whole-cell current-clamp recordings from striatal MSNs and L2 stellate neurons in the entorhinal cortex at 36.5-37.5°C showed that *TRPV3*$^{-/-}$ cells exhibited reduced intrinsic excitability, as evidenced by fewer spikes in response to 400-ms current steps, a hyperpolarized RMP, and a decrease in mEPSC frequency (Chen et al., 2022). These electrophysiological effects were also replicated using pharmacological inhibition of *TRPV3* with 50 μmol/L forsythoside B (Chen et al., 2022). Additionally, consistent with the idea that ischemic injury upregulates *TRPV3* expression, leading to intracellular Ca^{2+} overload and progressive cell death, inhibition of *TRPV3*, rather than N-methyl-D-aspartate (*NMDA*) receptors, protected against progressive cell death after stroke (Chen et al., 2022).

As STAY PNs and neurons that initiate spiking at fever temperature ("START" cells) are active at fever temperature, future research will focus on the molecular characterization of these cells

in the cortex and elsewhere in the brain at P12-14 and other ages. Interestingly, neurons that initiate spiking at fever temperature are more prevalent at P20-23 than at the earlier ages examined. *TRPV4* block caused a subset of PNs to initiate spiking at 39°C, suggesting that low *TRPV4* expression could define the population of START cells, at least at P12-14. Our initial characterization of $D1^+$ and $D2^+$ MSNs showed some overlap in the functional characteristics of STAY cells in L2/3 S1 cortex and the striatum, but further research is needed to determine whether a conserved set of channels functionally define these cell types across multiple brain regions.

Molecular characterization of STAY and START cell types may provide additional insights into their function within normal brain circuits. In response to specific experiences, selective subsets of neurons, known as "engrams," may become active to encode specific memories or behavioral responses (Lee et al., 2021). Alternatively, neurons that become active could initiate responses to specific stimuli, such as an increase in brain temperature. In this latter scenario, these neurons may be part of the brain's homeostatic response to temperature increases, while STAY neurons may play a critical role in facilitating ongoing cognitive functions during a fever. Future research into the molecular characterization of these cell types could offer opportunities to target and modulate their activity in a brain region-specific manner, potentially advancing treatments for fever-associated seizures or epilepsies, such as Dravet Syndrome (a genetic epilepsy typically initiating in early infancy) and febrile infection-related epilepsy syndrome (FIRES).

Acknowledgements

M.W.A. , R.F., and Y.S., designed, performed, interpreted and analyzed physiology experiments. M.W.A., and Y.S. designed, performed, and analyzed *ex vivo* electrophysiological

experiments. R.F. designed, performed, and analyzed *in vivo* electrophysiological experiments. M.W.A. wrote the paper. M.W.A and I.U. provided project supervision. We thank Dr. David Lovinger, Scientific Director of NIAAA, for his critical review of the manuscript.

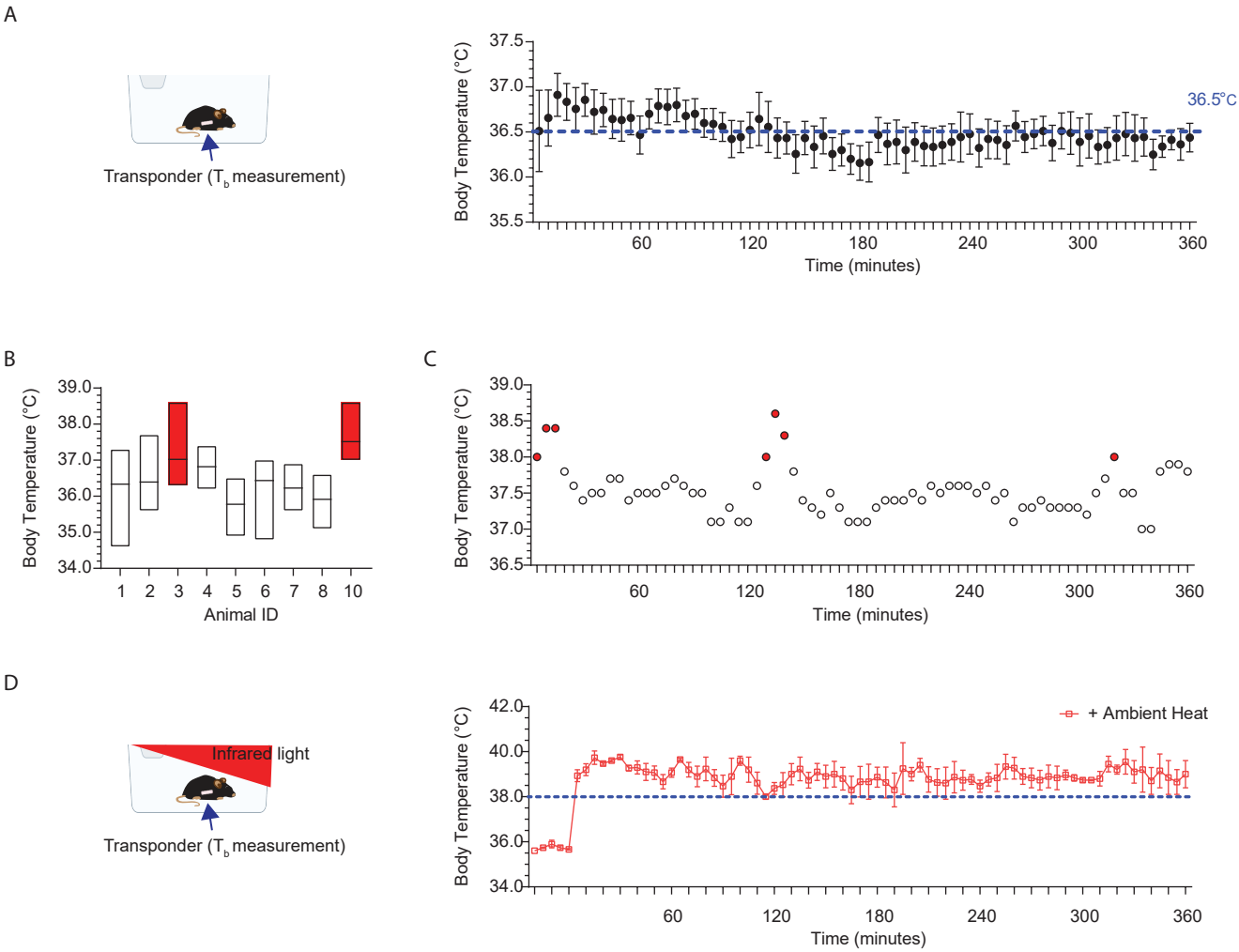

Figure 1: Body Temperature rises to fever levels during regular activity and exposure to higher ambient temperatures.

A. Left: Setup for recording mouse body temperature((T_b) at room temperature using an implanted transponder for non-invasive measurement. Right: Average T_b readings over 6 hours at 5-minute intervals for 10 mice. T_b typically hovers around 37°C during the day.

B. T_b may briefly elevate into fever range (shaded red bars) during regular daily activity. Median with upper and lower limits indicated.

C. T_b readings over 6 hours, at 5-minute intervals for animal 3 in Figure 1B. Shaded red dots indicate time points when T_b enters the fever range.

D. Left: Setup for T_b recordings during infrared light exposure. Right: T_b elevates into the fever range (>38°C) for extended durations, lasting minutes to hours. Average T_b readings over 6 hours at 5-minute intervals for 10 mice.

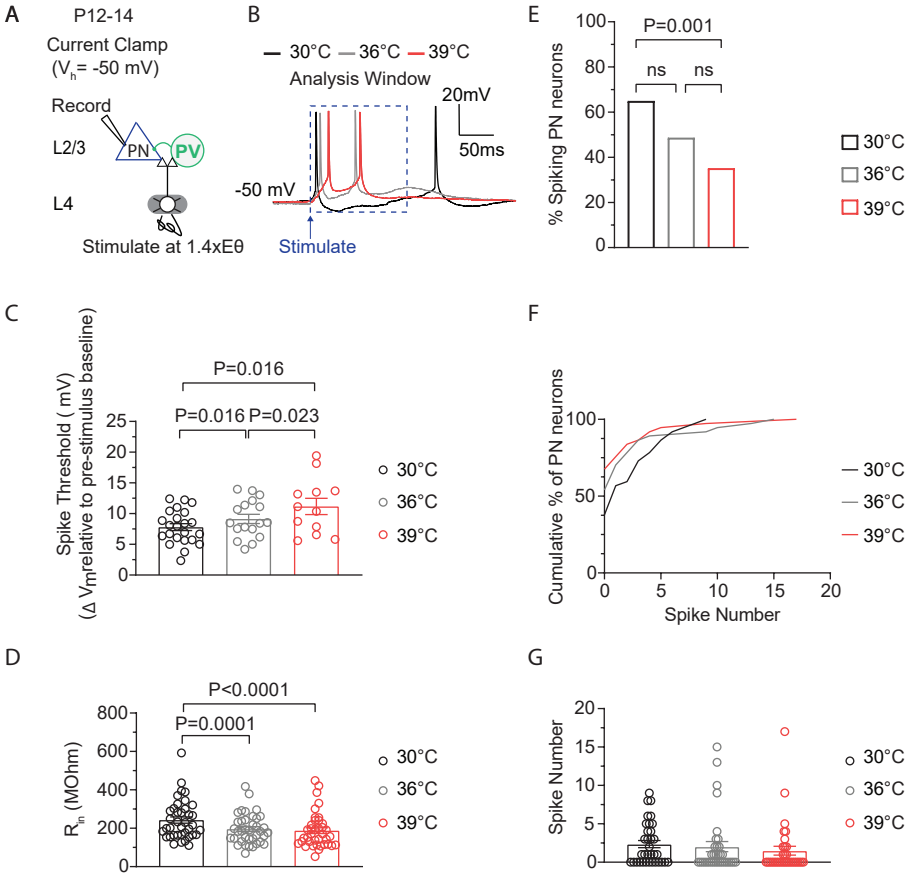

Figure 2: Spiking in P12-14 cortical excitatory pyramidal neurons remains stable as temperature enters the fever range.

A. Setup for recording L4-evoked postsynaptic potential and spiking in an excitatory pyramidal neuron (PN) at just-subthreshold V_m at 30°C, 36°C and 39°C in mouse primary somatosensory (S1) cortex.

B. Example traces of L4-evoked spikes in L2/3 PN during consecutive recordings at 30°C (black), 36°C (gray), and 39°C (red).

C. Depolarization required to reach spike threshold (ST) in L2/3 PNs during temperature elevations from 30°C to 39°C.

D. Same as (C) for input resistance (R_{in}).

E. Same as (C) for the percentage of spiking L2/3 PNs.

F. Same as in (C) for the spiking distribution.

G. Same as in (C) for the number of spikes.

Each data point represents an individual cell. 37 PNs recorded from 14 animals. Mean with standard error of the mean shown in C, D and G. Statistical significance assessed via one-way repeated measures ANOVA with Tukey's test at α=0.05.

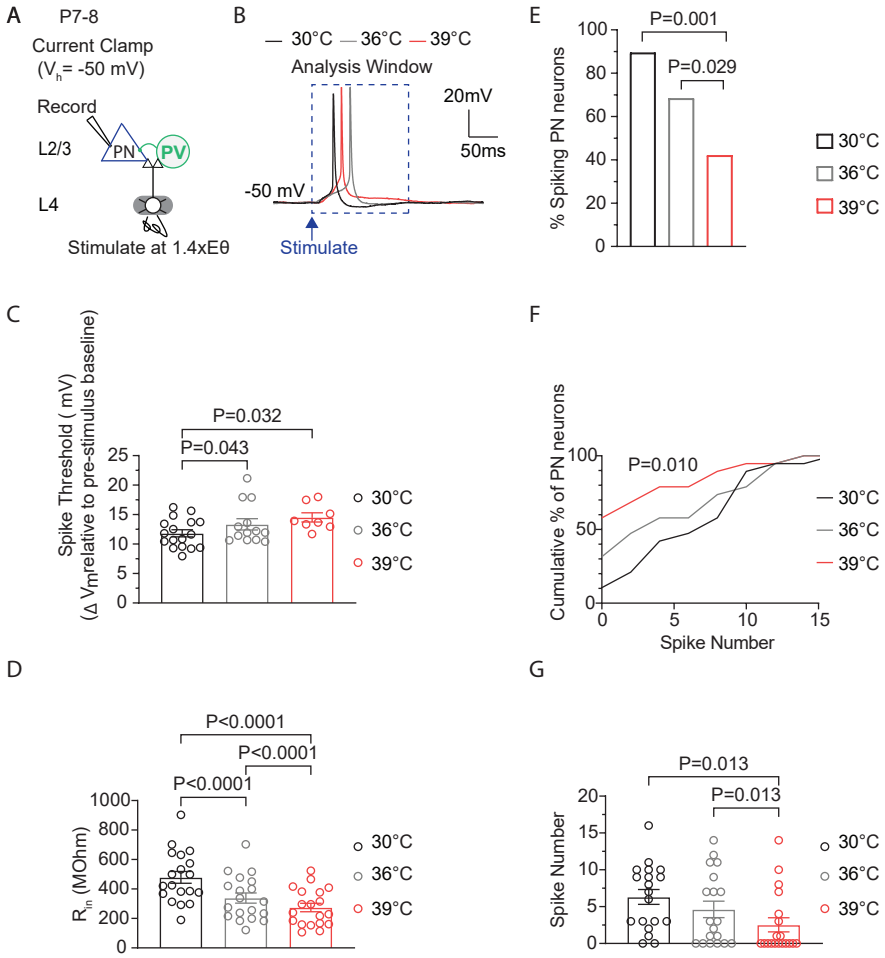

Figure 3: Spiking in P7-8 cortical excitatory pyramidal neurons decreases as temperature enters the fever range.

A. Setup for recording L4-evoked postsynaptic potential and spiking in an excitatory pyramidal neuron (PN) at just-subthreshold V_m at 30°C, 36°C and 39°C in mouse primary somatosensory (S1) cortex.

B. Example traces of L4-evoked spikes in L2/3 PN during consecutive recordings at 30°C (black), 36°C (gray), and 39°C (red).

C. Depolarization required to reach spike threshold (ST) in L2/3 PNs during temperature elevations from 30°C to 39°C.

D. Same as (C) for input resistance (R_{in}).

E. Same as (C) for the percentage of spiking L2/3 PNs.

F. Same as in (C) for the spiking distribution.

G. Same as in (C) for the number of spikes.

Each data point represents an individual cell. 19 PNs recorded from 5 animals. Mean with standard error of the mean shown in C, D and G. Statistical significance assessed via one-way repeated measures ANOVA with Tukey's test at α=0.05.

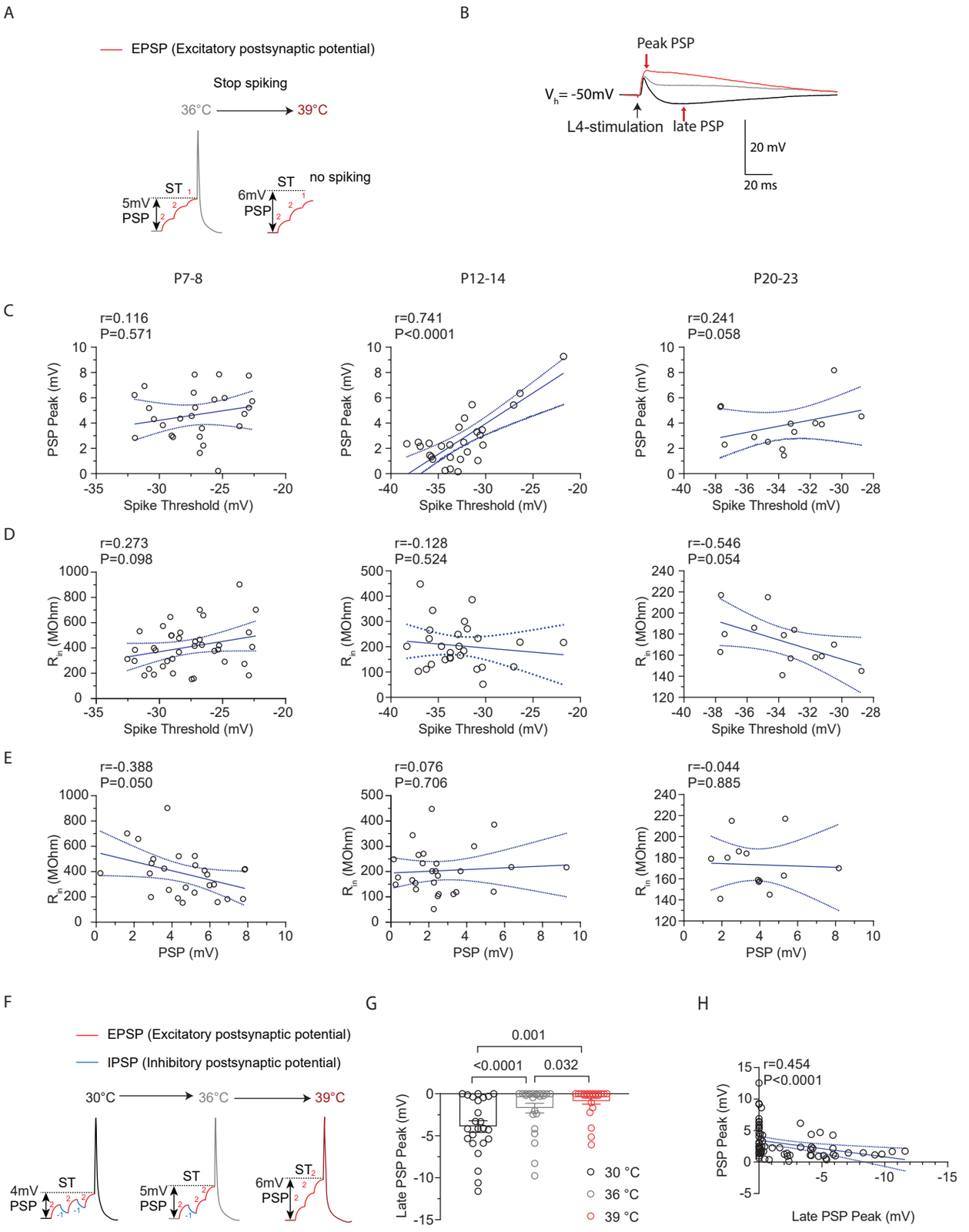

Figure 4: Increased depolarization at higher spike thresholds helps maintain stable spiking activity in cortical pyramidal neurons during temperature elevations.

A. Illustration demonstrating how temperature-induced changes in spike threshold make spiking more challenging for a neuron, requiring larger levels of depolarization to sustain spiking.

B. Example traces of L4-evoked postsynaptic potentials (PSPs) in L2/3 PN during consecutive recordings at 30°C (black), 36°C (gray), and 39°C (red).

C. Correlation of PSP peak versus spike threshold (ST). r = Pearson correlation coefficient with Deming linear regression.

D. Correlation of input resistance versus ST. r = Pearson correlation coefficient with simple linear regression.

E. Same as D but for input resistance versus PSP.

F. Illustration showing how temperature-induced loss in inhibition (blue IPSP) could lead to larger levels of depolarization. IPSPs typically bring the membrane potential away from the spike threshold.

G. The late PSP peak in L2/3 PNs during temperature elevations from 30°C to 39°C. Statistical significance was evaluated on log-transformed data using one-way repeated measures ANOVA with Tukey's test, with significance at α=0.05.

H. Same as D but for PSP versus Late PSP Peak.

r = Spearman correlation coefficient with simple linear regression.

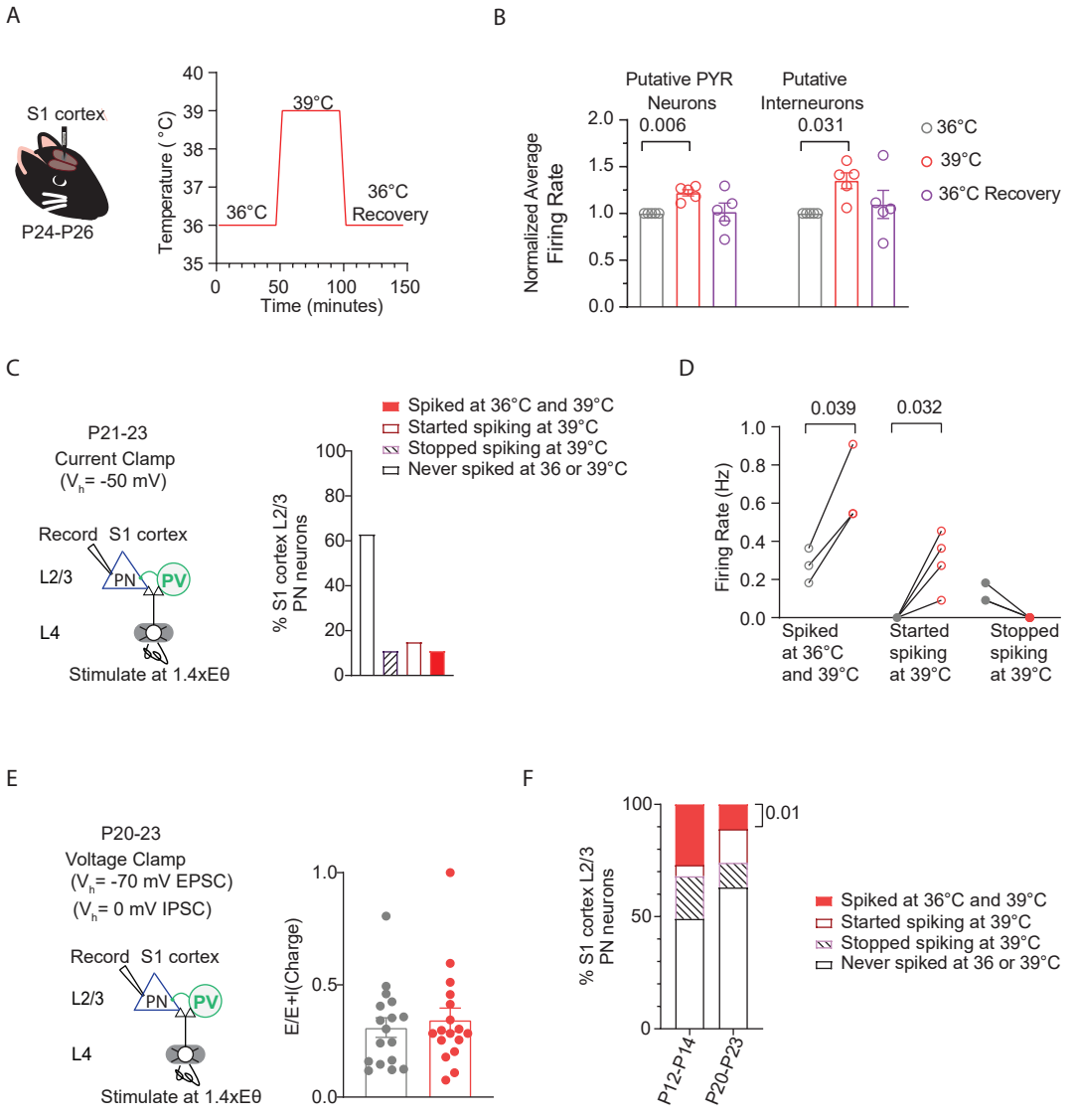

Figure 5: Cortical neurons that remain active at febrile temperatures spike at higher rates, but the excitatory-inhibitory balance remains unchanged.

A. Setup for *in vivo* recording of spiking in mouse S1 cortex during temperature increases from 36°C to 39°C and cooling back to 36°C.

B. Normalized firing rates from putative excitatory PNs and interneurons obtained from recordings in A.

C. Left: Setup for *ex vivo* recording of L4-evoked postsynaptic potential and spiking in a L2/3 PN at just-subthreshold V_m at 30°C, 36°C and 39°C in mouse S1 cortex. Right: Percent distribution for recorded PNs that never spiked, stopped spiking, stayed spiking, or started spiking during temperature increases from 36°C to 39°C.

D. L2/3 PN spiking activity in neurons that stayed spiking (left), started spiking (middle), and stopped spiking (right) upon temperature increases from 36°C to 39°C.

E. Left: Setup for *ex vivo* recording of L4-evoked excitatory and inhibitory postsynaptic currents (EPSCs and IPSCs, respectively). Right: The excitatory-inhibitory (E-I) balance (defined as E/E+I, the ratio of the EPSC to the total current (EPSC+IPSC) measurements during temperature increases from 36 to 39°C.

F. Activity distribution for *ex vivo* recorded neurons that never spiked, and those that stopped spiking, stayed spiking, or started spiking upon temperature increases from 36°C to 39°C. P-value = 0.01 indicates a significant increase in the fraction of neurons that stayed spiking during temperature increases from 36°C to 39°C (solid red bar).

In B,D and E, each data point represents an individual cell. Data collected from 5 animals (in B), 11 animals (in C,D), 7 animals (in E) and 9-14 animals (in F). Mean with standard error mean is indicated in B and E. Significance assessed by paired two-tailed t-test (D and E), one-way repeated measures ANOVA with Tukey's test (in B) and binomial test (in F). Significance at α=0.05.

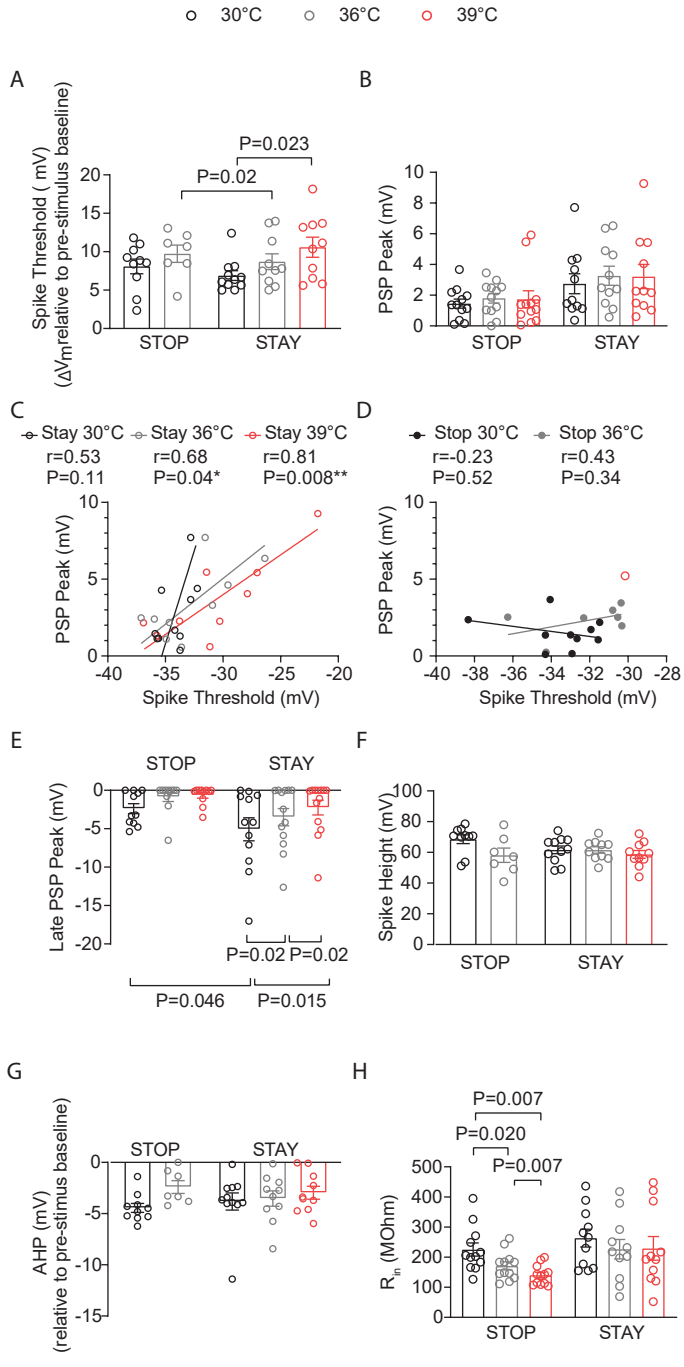

Figure 6: Excitatory pyramidal neurons that remain spiking with temperature elevations into fever range exhibit unique intrinsic properties.

Neurons that spiked at all temperatures (30°C, 36°C, and 39°C) are STAY PNs, while those that stopped spiking at 36°C or 39°C are STOP neurons.

A. Depolarization required to reach spike threshold (ST) in STOP and STAY L2/3 PNs during temperature elevations from 30°C to 39°C.

B. Same as (A) for L4-evoked postsynaptic potentials (PSPs)

C. Correlation of PSP peak versus ST in STAY L2/3 PNs at 30°C, 36°C, and 39°C. r = Pearson correlation coefficient with Deming linear regression.

D. Same as (C) for STOP cells.

E. Same as (A) for the L4-evoked late PSP peak.

F. Same as (A) for spike height.

G. Same as (A) for spike afterhyperpolarization (AHP).

H. Same as (A) for input resistance.

Each data point represents an individual cell in A-H. Data collected from 14 animals. Mean with standard error mean is indicated in A-B and E-H. Significance assessed by one- and two-way repeated measures ANOVA with Tukey's or Sidak post-hoc test, or paired t-test at α=0.05.

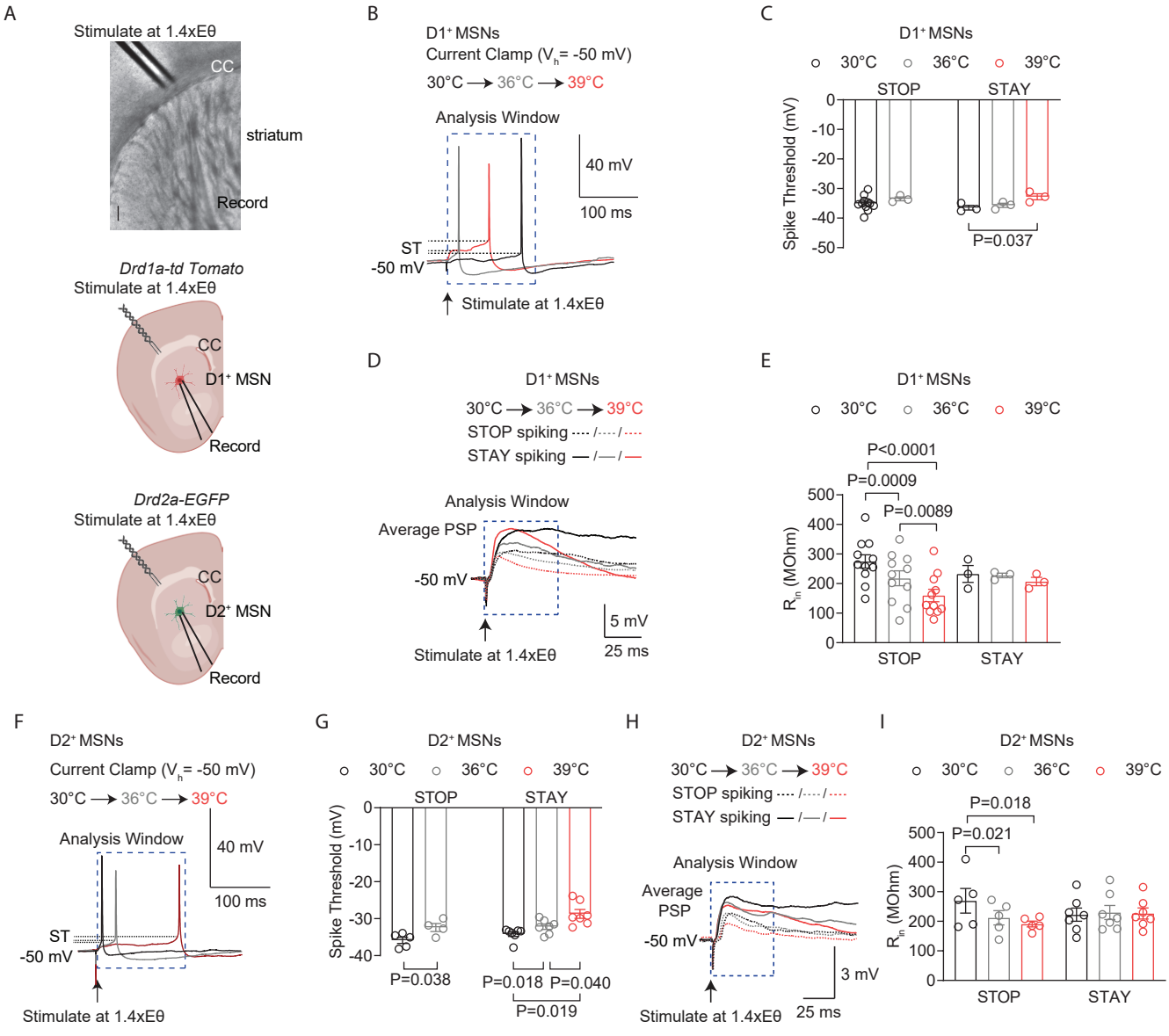

Figure 7: Medium spiny neurons (MSNs) that remain spiking with temperature elevations into fever range exhibit unique intrinsic properties.

Neurons that spiked at all temperatures (30°C, 36°C, and 39°C) are STAY MSNs, while those that stopped spiking at 36°C or 39°C are STOP MSNs.

A. Setup for recording evoked spiking in MSNs expressing dopamine (D)1-type receptors (i.e. $D1^+$ MSNs) or D2-type receptors (i.e. $D2^+$ MSNs).

B. Example traces of evoked spikes in $D1^+$ MSN during consecutive recordings at 30°C (black), 36°C (gray), and 39°C (red).

C. Depolarization required to reach spike threshold (ST) in STOP and STAY $D1^+$ MSNs during temperature elevations from 30°C to 39°C.

D. Summed trace (B) for evoked postsynaptic potentials (PSPs).

E. Same as (C) for input resistance.

F. Same as (B) for evoked spikes in $D2^+$ MSNs.

G. Same as (C) for ST in $D2^+$ MSNs.

H. Same as (B) for evoked PSPs in $D2^+$ MSNs.

I. Same as (C) for input resistance in $D2^+$ MSNs

Each data point represents an individual cell in C-D and G and I. Summed trace from all recordings is indicated in D and H. Data collected from 6 animals in C-E and 4 animals in F-G . Mean with standard error mean is indicated in C-D and F-G. Significance assessed by one- and two-way repeated measures ANOVA with Tukey's or Sidak post-hoc test, or paired t-test at $\alpha=0.05$.

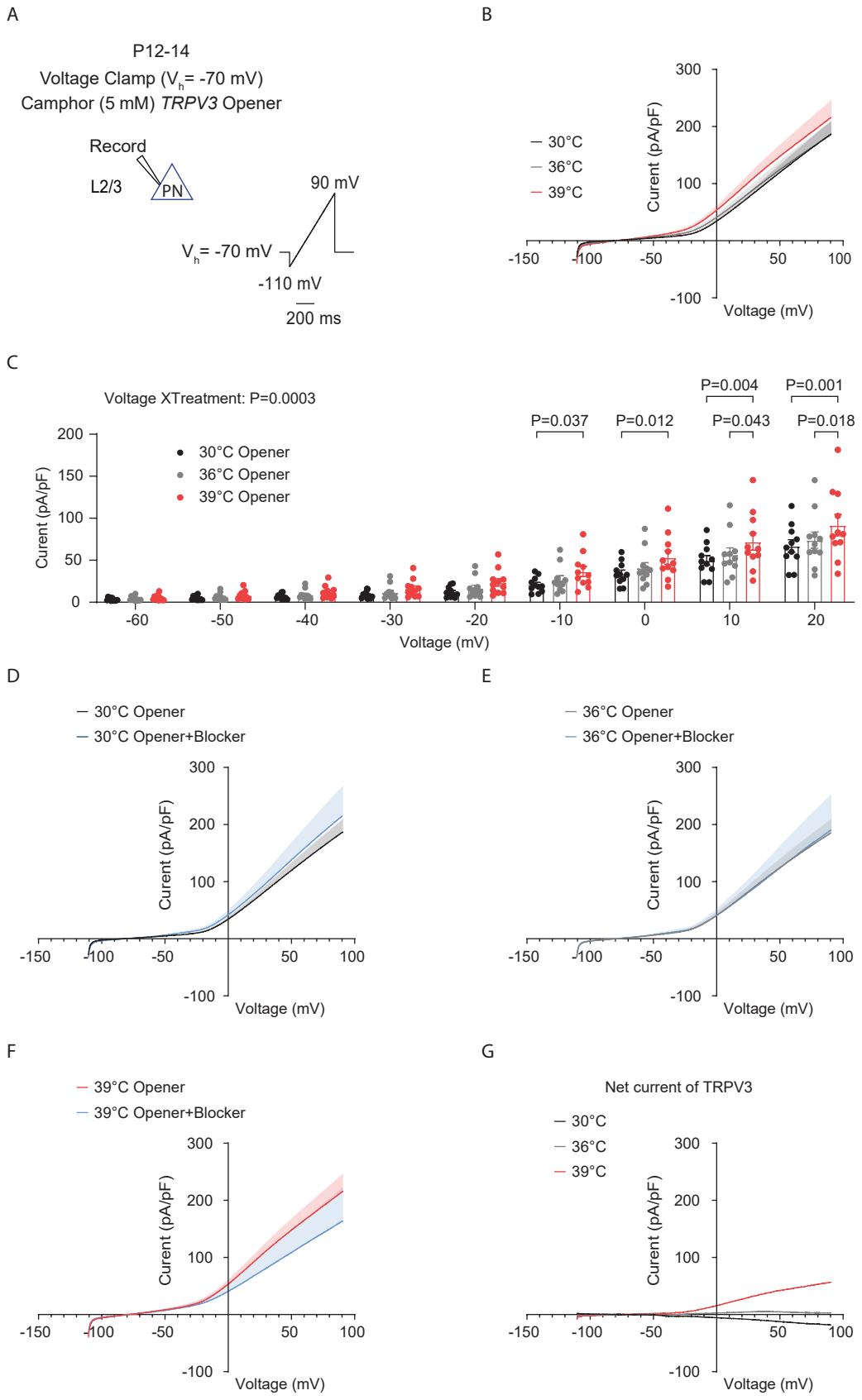

Figure 8: Temperature elevations in fever range increase *TRPV3* currents in cortical pyramidal neurons.

A. Setup for recording whole-cell *TRPV3* currents at 30°C (black), 36 °C (grey) and 39°C (red). in cortical excitatory pyramidal neurons (PNs) with bath application of camphor (5mM), a *TPRV3* agonist.

B. Current density-voltage (I-V) relationship of *TRPV3* currents at 30°C (black), 36 °C (grey) and 39°C (red) in WT mice: 11 cells from 4 mice.

C. Scatter dot plots of the current density-voltage measurements.

D. Current density-voltage (I-V) relationship of *TRPV3* currents at 30°C (black) in the presence of camphor (5mM), a *TPRV3* agonist, or camphor (5mM) + *TRPV3* blocker (Forsythoside B, 50 μM) (blue).

E. Same as (**D**) but for 36°C.

F. Same as (**D**) but for 39°C.

G. Current density-voltage (I-V) plot showing the net TRPV3 current (opener – (opener+ blocker) condition).

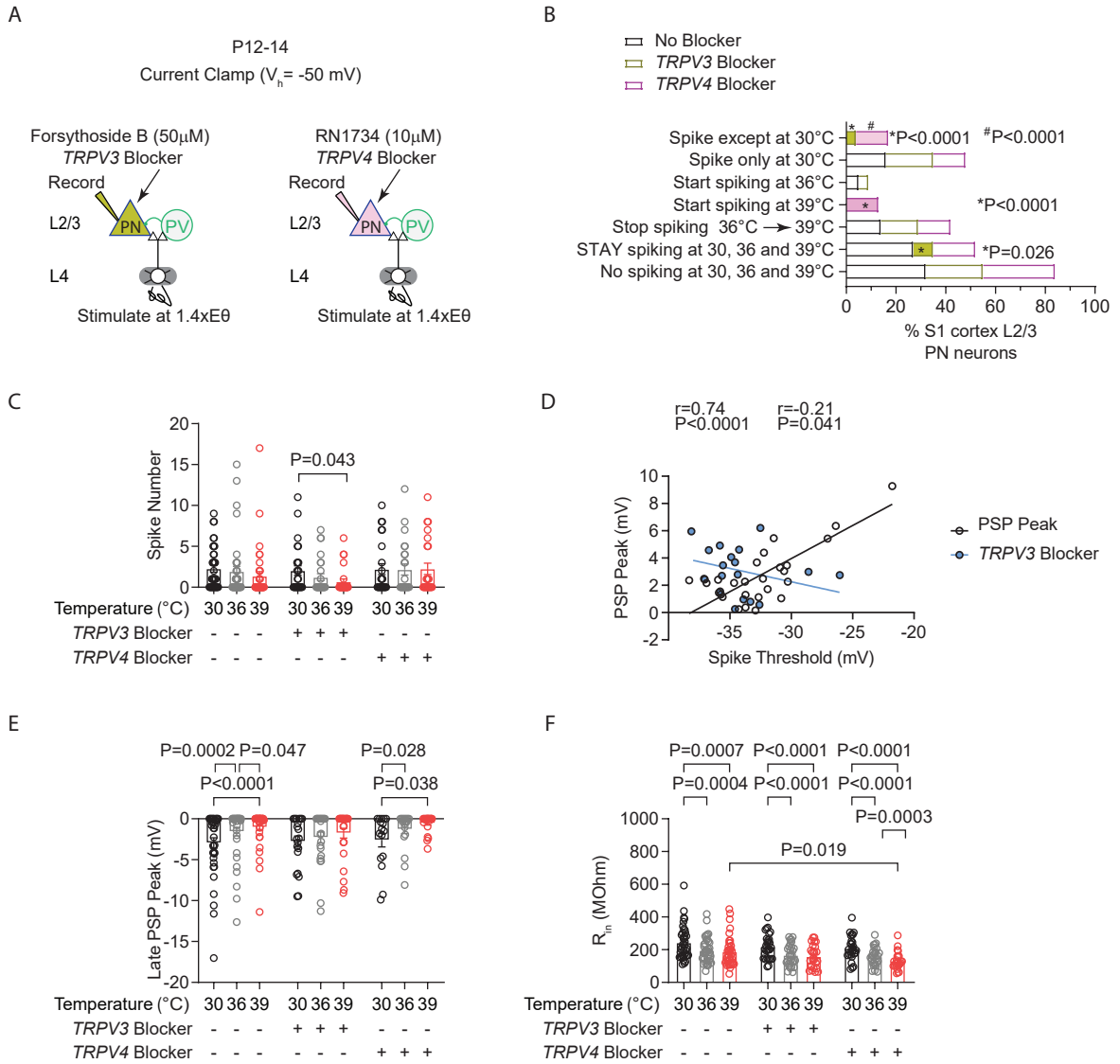

Figure 9: Inhibiting TRPV3, but not TRPV4 channels, significantly reduced the population of STAY pyramidal neurons and spiking levels at fever temperature.

A. Setup for recording L4-evoked postsynaptic potential and spiking in an excitatory pyramidal neuron (PN) with an intracellular blocker of TRPV3 channels (Forsythoside B, 50 μM) (left) or TRPV4 channels (RN1734, 10 μM) (right) at just-subthreshold V_m at 30°C, 36°C, and 39°C in mouse S1 cortex.

B. Percentages of cell types obtained from experiment in A.

C. Evoked spikes in L2/3 PNs during temperature elevations to 30°C, 36°C, and 39°C with TRPV3 (Forsythoside B, 50 μM) or TRPV4 (RN1734, 10 μM) blockers.

D. Correlation of PSP peak versus spike threshold (ST). r = Pearson correlation coefficient with Deming linear regression.

E. Same as (C) for the L4-evoked late PSP peak.

F. Same as (C) for input resistance.

Each data point represents an individual cell in C, E and F. Data collected from 26 cells in 7 animals for TRPV3 blocker, 24 cells in 6 animals for TRPV4 blocker, and 37 cells from 14 animals for no block condition. Mean with standard error mean is indicated in C, E and F. Significance assessed by one- and two-way repeated measures ANOVA with Tukey's or Sidak post-hoc test at α=0.05.

Materials and Methods

Animals

All experimental procedures were performed in accordance with the National Institutes of Health guidelines for care and use of laboratory animals and the EC Council Directive of September 22, 2010 (2010/63/EU). All experiemnts were approved by the Animal Care and Use Committee of the National Institute on Alcohol Abuse and Alcoholism (NIAAA) (Protocol # LIN-MA-1) and the Animal Care Committee of the Research Centre for Natural Sciences (RCNS) and by the National Food Chain Safety Office of Hungary (license number: PE/EA/1004-5/2021). Mice were housed under standard conditions with ad libitum access to food and water, under a 12-h light/dark cycle. The following mouse strains were obtained from The Jackson Laboratory (JAX) or the Mutant Mouse Resource and Research Center (MMRRC) and bred in onsite Colonies at the NIAAA or RCNS: C57BL/6J (JAX 000664), FVB/N mice(JAX 004828), Drd2-EGFP **(**MMRRC: 000230-UNC) (Gong et al., 2003); Drd1-tdTomato (JAX 016204) (Ade et al., 2011). The day of birth was denoted as postnatal day (P)1. Both male and female mice were used for body temperature (T_b) recordings and electrophysiological experiments.

Body Temperature Measurements

All mice used for body temperature (T_b) recordings were implanted with sterile IPTT-300 Implantable Programmable Temperature transponders (Bio Medic Data Systems, LLC) at 2 weeks of age. The injection site was pre-cleaned with a betadine solution, and the sterile transponders were injected subcutaneously using a pre-loaded 12-gauge syringe into animals anesthetized with 4-5% isoflurane. The injection site was on the left side, approximately 11 cm from the base of the hip, with the animal in the prone position. Post-implantation, the mice were able to move, eat, and drink autonomously, with no adverse phenotypes noted. T_b recording commenced at least 5 days after injection. Prior to recording, mice were brought into the

procedure room and allowed to habituate for 1 hour. T_b was recorded every 5 minutes for 6 hours using an IPTT-300 Implantable Programmable Temperature reader (DAS-8027) in a 37L x 16W x 13H cm cage. T_b was recorded in the presence (Figure 1D) or absence (Figure 1A-C) of infrared light. Infrared light exposure was provided via a 250-W temperature-controlled infrared lamp (catalog #50320, Stoelting), set to 32.5-33.5 °C. The lamp was positioned ~15 cm above the cage, and the ambient temperature was monitored every 5 minutes (Figure 1D).

Slice Preparation

Using standard methods, acute primary somatosensory cortex (S1) slices (350 µm thick) from P7-8, P12-14, or P20-23 mice were cut in the "across-row" plane, oriented 35° toward coronal from midsagittal (Antoine et al., 2019). Striatal slices (350 µm thick) were cut in the coronal plane at bregma (+1.3 mm to +0.5 mm) from P12-14 mice. The cutting solution contained (in mM): 85 NaCl, 75 sucrose, 25 D- (+)-glucose, 4 $MgSO_4$, 2.5 KCI, 1.25 NaH_2PO_4, 0.5 ascorbic acid, 25 $NaHCO_3$, 0.5 $CaCl_2$. Once cut, slices were transferred to a submerged-style holding chamber containing standard Ringer's solution (in mM: 119 NaCl, 2.5 KCI, 1.3 $MgSO_4$, 1 NaH_2PO_4, 26.2 $NaHCO_3$, 11 D-(+)-glucose and 2.5 $CaCl_2$) and then incubated at 32°C for 30 minutes. Both solutions were at neural pH (i.e., 7.3), 300 mOsm, and saturated with 95% O_2 and 5% CO_2. Slices were kept at room temperature for at least 30 minutes before being transferred to a submerged recording chamber.

In Vitro Physiology

Whole-cell current-clamp recordings were made from pyramidal neurons (PNs) visually identified via infrared DIC optics, or from $D1^+$ and $D2^+$ MSNs identified via the expression of the fluorescent proteins *tdTomato* and *EGFP*, respectively. Physiological verification for regular spiking was done in current clamp. Recordings were made using 3-6 MΩ micropipettes

containing (in mM):116 K gluconate, 20 HEPES, 6 KCl, 2 NaCl, 0.5 EGTA, 4MgATP, 0.3 NaGTP, 10 Na phosphocreatine, with a Multiclamp 700B amplifier (Molecular Devices, Sunnyvale, CA). Where applicable, forsythoside B (50 µM, *TRPV3* blocker, Millipore Sigma Cat #: PHL83313) or RN1734 (10 µM, *TRPV4 blocker*, Tocris Bioscience Cat #: 3746/25) was added to the internal solution. Camphor (MedChem, Cat. No: HY-N0808) was added to the bath solution for experiments in figure 8.

Signals were low-pass filtered (2-6 kHz) and digitized (10-20 kHz). Perfusate temperature for all in vitro experiments was regulated by a PC-connected Peltier heater (SM-4600, Scientifica, UK) and temperature controller (Linlab2, Scientifica, UK), with a high-accuracy, low-noise temperature control system, containing both a built-in temperature sensor and bath sensor for accurate feedback. ACSF flow rates of ~3 ml/min were used to facilitate efficient heating/cooling.

To determine the effect of temperature on an activated cortical network, layer 4-evoked spiking was quantified during perfusate temperature increases from 30°C to 36°C, and then to fever range (~39°C) while recording membrane potential. The slicing plane facilitated clear identification of whisker barrel columns, and neuronal activity was evoked by stimulating the barrel center using a bipolar electrode (0.2 ms pulses) at a stimulation of 1.4 Eθ. Eθ is defined as the minimal intensity that evoked a consistent excitatory postsynaptic current (EPSC) during more than 3 of 5 consecutive sweeps with 10 s ISI (Antoine et al., 2019). Eθ was determined in voltage clamp for each recorded cell prior to recording PSPs and spiking in current clamp. A new brain slice was used for each recording. L4- evoked feedforward post synaptic potentials (PSPs) and spiking were recorded in single L2/3 PNs from a pre-stimulus baseline membrane potential (V_m) of -50 mV. This V_m, just below spike threshold, was selected to mimic *in vivo*

conditions, as PNs *in vivo* can reside within this V_m range during whisker exploration of objects or surfaces (Yamashita et al., 2013). Similarly, $D1^+$ and $D2^+$ MSNs in the dorsolateral striatum, which respond to whisker stimulation, can reach similar V_m levels during whisking epochs or other sensory stimulation (Druart et al., 2024; de la Torre-Martinez et al., 2023). Evoked spikes were analyzed over a 150-ms interval, starting 2-3 ms post-stimulus, for 11 sweeps at 10 s inter-sweep interval (ISI). Spike threshold was defined as the membrane potential (V_m) at which the second derivative of V_m was >5 SDs above the pre-stimulus period.

Animal Surgery and Electrophysiological Recordings

Experiments were done under general anesthesia where five mice (age, P24-26; body weight, 7-10 g; both genders) received an intraperitoneal injection of ketamine (100 mg/kg) and xylazine (10 mg/kg). Regular doses of the ketamine/xylazine cocktail were given intramuscularly to maintain the depth of anesthesia during the experimental sessions. Up until the thermal fever protocol started, the T_b of the animals was kept at 36°C using a homeothermic heating pad connected to a temperature controller (Supertech, Pécs, Hungary). To measure the internal body temperature, a Type T thermocouple microprobe (MT-29/5; Physitemp Instruments, Clifton, NJ, USA) was placed in the rectum of the animal. The microprobe has a shaft diameter of 330 µm, a time constant of 0.025 second and 0.1°C accuracy.

To perform high-density extracellular electrophysiological recordings, mice were placed in a stereotaxic frame (David Kopf Instruments, Tujunga, CA, USA), then two circular craniotomies (~1.5 mm in diameter) were made with a dental drill above the left and right barrel cortices. The craniotomies were centered at the following stereotaxic coordinates: anterior-posterior (AP): −1.0 mm; medial-lateral (ML): 3.5 mm (with respect to the bregma; Paxinos and Franklin 2001). Two commercially available Neuropixels 1.0 silicon probes (imec, Leuven, Belgium; Jun et al.,

2017) mounted on two motorized stereotaxic micromanipulators (Neurostar, Tubingen, Germany) were implanted into the brain, one into the left and the other into the right barrel cortex, to a depth of 1.5 mm. An insertion speed of 2 µm/s was used to decrease the mechanical trauma caused by the probe insertion (Fiáth et al. 2019).

In order for the probe tracks to be perpendicular to cortical layers, the probes were inserted at an angle of 20 degrees from vertical. The dura mater in the craniotomy was left intact, except when it was too thick and thus the silicon probe could not pierce through this layer (which was indicated by significant probe buckling; n = 3 insertions). In these cases a 36 gauge, slightly bent needle was used to carefully cut the dura above the targeted cortical area. After the probe reached its final insertion depth, to allow the brain tissue to settle, we waited at least 10 minutes before electrophysiological recording was started. Spiking activity of cortical neurons (action potential band, 300–10.000 Hz) was recorded on 384 channels (768 channels in total for the two probes), with a sampling rate of 30 kHz/channel and with a gain of 500 (yielding a resolution of 2.34 µV per bit). Data were acquired using the SpikeGLX open-source software (http://billkarsh.github.io/SpikeGLX/).

A common stainless steel wire inserted into the neck muscle of the animal served as the external reference and ground electrode. To avoid the dehydration of the cortex, the skull and the craniotomy was kept moist during the whole experiment using body temperature, sterile physiological saline solution and Gelaspon. Before starting the experimental protocol, manual whisker stimulation (by repetitively touching the whiskers of the animal with a cotton swab) was used to verify the recording position. In all cases (n = 10 probe insertions), we detected strong whisker-evoked neuronal activity.

Thermal Fever Protocol during Electrophysiological Recordings

First, we recorded cortical activity for 45 minutes at ~36°C body temperature ("baseline " period), then the body temperature of the animal was elevated with the aid of the heating pad and a power bank with warming capability which was placed next to the mouse. The body temperature was increased from 36°C to 39°C in about 5 minutes (~0.01°C/s). The elevated body temperature was maintained for 45 minutes ("thermal fever " period). Next, we turned off the heating until the T_b reached physiological temperatures (36°C; ~5 min; ~0.01°C/s). Cortical activity was recorded for another 45 minutes at 36°C body temperature ("recovery " period). Continuous recordings with a total duration of 145 minutes were obtained for each mouse.

Spike Sorting and Data Analysis

To extract cortical single-unit activity, spike sorting was performed with Kilosort2 (https://github.com/MouseLand/Kilosort; Pachitariu et al., 2016a, 2016b) using the default parameter set (available in the StandardConfig.m file). Channels containing activity acquired by recording sites located outside the cortex were removed before spike sorting (usually ~130 channels/probe recorded from the barrel cortex). The list of single unit clusters generated by Kilosort2 was visually inspected to remove units considered as noise (e.g., units with abnormal spike waveform shapes) or multi-unit activity (e.g., clusters with a contaminated refractory period). Manual curation of the Kilosort2 results was done with the Phy Python library, which provides a graphical user interface for interactive visualization of high-density data and supplies operations for merging, splitting and marking of clusters (https://github.com/cortex-lab/phy; Rossant et al., 2016). In this dataset, we aimed to keep only those single units which had at least 900 spikes (>~0.1 Hz firing rate), a clear refractory period, a consistent waveform shape and whose spikes were present throughout the 145-minute-long recording.

Following manual curation, based on their spike waveform duration, the selected single units (n = 633) were separated into putative inhibitory interneurons and excitatory principal cells (Barthó

et al., 2004). The spike duration was calculated as the time difference between the trough and the subsequent waveform peak of the mean filtered (300 – 6000 Hz bandpassed) spike waveform. Durations of extracellularly recorded spikes showed a bimodal distribution (Hartigan's dip test; $p < 0.001$) characteristic of the neocortex with shorter durations corresponding to putative interneurons (narrow spikes) and longer durations to putative principal cells (wide spikes). Next, k-means clustering was used to separate the single units into these two groups, which resulted in 140 interneurons (spike duration < 0.6 ms) and 493 principal cells (spike duration > 0.6 ms), corresponding to a typical 22% - 78% (interneuron – principal) cell ratio. Finally, the firing rates of neurons were computed separately during the three distinguished periods (baseline, thermal fever and recovery). To decrease the effect of transient changes (e.g., tissue recovery during the baseline period or the short-term effect of heating during the thermal fever period), for each 45-minute-long period, we used only the last 25-minutes to calculate the mean firing rates of neurons.

Statistics

Statistical analyses were conducted using Prism 9.0 (GraphPad). For experiments, at least 3 mice from a minimum of 2 separate litters were used, with littermates typically included across the age groups P7-8, P12-14, and P20-23. Non-Gaussian data were either log-transformed for parametric testing or subjected to nonparametric tests, as specified in the results and figure legends. Significance was consistently reported at $\alpha = 0.05$. Details on the statistical tests used are provided in the figure captions.

References

Ade, K. K., Y. Wan, M. Chen, B. Gloss, and N. Calakos.(2011) An Improved Bac Transgenic Fluorescent Reporter Line for Sensitive and Specific Identification of Striatonigral

Medium Spiny Neurons. *Front Syst Neurosci* 5: 32. https://doi.org/10.3389/fnsys.2011.00032.
Antoine, M. W., T. Langberg, P. Schnepel, and D. E. Feldman.(2019) Increased Excitation-Inhibition Ratio Stabilizes Synapse and Circuit Excitability in Four Autism Mouse Models. *Neuron* 101, no. 4: 648-61 e4. https://doi.org/10.1016/j.neuron.2018.12.026.
Baram, T. Z., A. Gerth, and L. Schultz.(1997) Febrile Seizures: An Appropriate-Aged Model Suitable for Long-Term Studies. *Brain Res Dev Brain Res* 98, no. 2: 265-70. https://doi.org/10.1016/s0165-3806(96)00190-3.
Bartho, P., H. Hirase, L. Monconduit, M. Zugaro, K. D. Harris, and G. Buzsaki.(2004) Characterization of Neocortical Principal Cells and Interneurons by Network Interactions and Extracellular Features. *J Neurophysiol* 92, no. 1: 600-8. https://doi.org/10.1152/jn.01170.2003.
Bhatia, A., S. Moza, and U. S. Bhalla.(2019) Precise Excitation-Inhibition Balance Controls Gain and Timing in the Hippocampus. *Elife* 8. https://doi.org/10.7554/eLife.43415.
Brown, P. L., R. A. Wise, and E. A. Kiyatkin.(2003) Brain Hyperthermia Is Induced by Methamphetamine and Exacerbated by Social Interaction. *J Neurosci* 23, no. 9: 3924-9. https://doi.org/10.1523/JNEUROSCI.23-09-03924.2003.
Campbell, I.(2011) Body Temperature and Its Regulation. *Anaesthesia and Intensive Care Medicine* 12, no. 6: 240-44. https://doi.org/DOI 10.1016/j.mpaic.2011.03.002.
Caterina, M. J.(2007) Transient Receptor Potential Ion Channels as Participants in Thermosensation and Thermoregulation. *Am J Physiol Regul Integr Comp Physiol* 292, no. 1: R64-76. https://doi.org/10.1152/ajpregu.00446.2006.
Chen, X., J. Zhang, and K. Wang.(2022) Inhibition of Intracellular Proton-Sensitive Ca(2+)-Permeable Trpv3 Channels Protects against Ischemic Brain Injury. *Acta Pharm Sin B* 12, no. 5: 2330-47. https://doi.org/10.1016/j.apsb.2022.01.001.
de la Torre-Martinez, R., M. Ketzef, and G. Silberberg.(2023) Ongoing Movement Controls Sensory Integration in the Dorsolateral Striatum. *Nat Commun* 14, no. 1: 1004. https://doi.org/10.1038/s41467-023-36648-0.
Druart, M., M. Kori, C. Chaimowitz, C. Fan, and T. Sippy.(2024) Cell-Type Specific Auditory Responses in the Striatum Are Shaped by Feed Forward Inhibition. *bioRxiv*. https://doi.org/10.1101/2024.05.09.592848.
Dube, C. M., T. Ravizza, M. Hamamura, Q. Zha, A. Keebaugh, K. Fok, A. L. Andres*, et al.*(2010) Epileptogenesis Provoked by Prolonged Experimental Febrile Seizures: Mechanisms and Biomarkers. *J Neurosci* 30, no. 22: 7484-94. https://doi.org/10.1523/JNEUROSCI.0551-10.2010.
Fiath, R., A. L. Marton, F. Matyas, D. Pinke, G. Marton, K. Toth, and I. Ulbert.(2019) Slow Insertion of Silicon Probes Improves the Quality of Acute Neuronal Recordings. *Sci Rep* 9, no. 1: 111. https://doi.org/10.1038/s41598-018-36816-z.
Gong, S., C. Zheng, M. L. Doughty, K. Losos, N. Didkovsky, U. B. Schambra, N. J. Nowak*, et al.*(2003) A Gene Expression Atlas of the Central Nervous System Based on Bacterial Artificial Chromosomes. *Nature* 425, no. 6961: 917-25. https://doi.org/10.1038/nature02033.
Hankenson, F. C., J. O. Marx, C. J. Gordon, and J. M. David.(2018) Effects of Rodent Thermoregulation on Animal Models in the Research Environment. *Comp Med* 68, no. 6: 425-38. https://doi.org/10.30802/AALAS-CM-18-000049.
Hardingham, N. R., and A. U. Larkman.(1998) Rapid Report: The Reliability of Excitatory Synaptic Transmission in Slices of Rat Visual Cortex in Vitro Is Temperature Dependent. *J Physiol* 507 (Pt 1), no. Pt 1: 249-56. https://doi.org/10.1111/j.1469-7793.1998.249bu.x.

Holtzman, D., K. Obana, and J. Olson.(1981) Hyperthermia-Induced Seizures in the Rat Pup: A Model for Febrile Convulsions in Children. *Science* 213, no. 4511: 1034-6. https://doi.org/10.1126/science.7268407.

Jun, J. J., N. A. Steinmetz, J. H. Siegle, D. J. Denman, M. Bauza, B. Barbarits, A. K. Lee*, et al.*(2017) Fully Integrated Silicon Probes for High-Density Recording of Neural Activity. *Nature* 551, no. 7679: 232-36. https://doi.org/10.1038/nature24636.

Kanju, P., and W. Liedtke.(2016) Pleiotropic Function of Trpv4 Ion Channels in the Central Nervous System. *Exp Physiol* 101, no. 12: 1472-76. https://doi.org/10.1113/EP085790.

Kashio, M., and M. Tominaga.(2022) Trp Channels in Thermosensation. *Curr Opin Neurobiol* 75: 102591. https://doi.org/10.1016/j.conb.2022.102591.

Kim, J. A., and B. W. Connors.(2012) High Temperatures Alter Physiological Properties of Pyramidal Cells and Inhibitory Interneurons in Hippocampus. *Front Cell Neurosci* 6: 27. https://doi.org/10.3389/fncel.2012.00027.

Kiyatkin, E. A.(2019) Brain Temperature and Its Role in Physiology and Pathophysiology: Lessons from 20 Years of Thermorecording. *Temperature (Austin)* 6, no. 4: 271-333. https://doi.org/10.1080/23328940.2019.1691896.

Lee, J., J. Urban-Ciecko, E. Park, M. Zhu, S. E. Myal, D. J. Margolis, and A. L. Barth.(2021) Fosgfp Expression Does Not Capture a Sensory Learning-Related Engram in Superficial Layers of Mouse Barrel Cortex. *Proc Natl Acad Sci U S A* 118, no. 52. https://doi.org/10.1073/pnas.2112212118.

Miller, D. J., and P. E. Fort.(2018) Heat Shock Proteins Regulatory Role in Neurodevelopment. *Front Neurosci* 12: 821. https://doi.org/10.3389/fnins.2018.00821.

Moqrich A., S. W. Hwang, T. J. Earley, M. J. Petrus, A. N. Murray, K. S. Spencer, M. Andahazy, G. M. Story, and A. Patapoutian.(2005) Impaired Thermosensation in Mice Lacking Trpv3, a Heat and Camphor Sensor in the Skin. *Science* 307, no. 5714: 1468-72. https://doi.org/10.1126/science.1108609.

Moussaieff, A., N. Rimmerman, T. Bregman, A. Straiker, C. C. Felder, S. Shoham, Y. Kashman*, et al.*(2008) Incensole Acetate, an Incense Component, Elicits Psychoactivity by Activating Trpv3 Channels in the Brain. *FASEB J* 22, no. 8: 3024-34. https://doi.org/10.1096/fj.07-101865.

Oakley, J. C., F. Kalume, F. H. Yu, T. Scheuer, and W. A. Catterall.(2009) Temperature- and Age-Dependent Seizures in a Mouse Model of Severe Myoclonic Epilepsy in Infancy. *Proc Natl Acad Sci U S A* 106, no. 10: 3994-9. https://doi.org/10.1073/pnas.0813330106.

Pachitariu, M., N. Steinmetz, S. Kadir, M. Carandini, and K. Harris.(2016) Fast and Accurate Spike Sorting of High-Channel Count Probes with Kilosort. *Advances in Neural Information Processing Systems 29 (Nips 2016)* 29.

Pachitariu, Marius, Nicholas A. Steinmetz, Shabnam N. Kadir, Matteo Carandini, and Harris %J bioRxiv Kenneth D.(2016) Kilosort: Realtime Spike-Sorting for Extracellular Electrophysiology with Hundreds of Channels.

Paxinos G, Franklin KBJ. (2001)The Mouse Brain in Stereotaxic Coordinates. Academic Press, London, UK: Elsevier Science, 2001.

Rossant, C., S. N. Kadir, D. F. M. Goodman, J. Schulman, M. L. D. Hunter, A. B. Saleem, A. Grosmark*, et al.*(2016) Spike Sorting for Large, Dense Electrode Arrays. *Nat Neurosci* 19, no. 4: 634-41. https://doi.org/10.1038/nn.4268.

Shibasaki, K., M. Suzuki, A. Mizuno, and M. Tominaga.(2007) Effects of Body Temperature on Neural Activity in the Hippocampus: Regulation of Resting Membrane Potentials by Transient Receptor Potential Vanilloid 4. *J Neurosci* 27, no. 7: 1566-75. https://doi.org/10.1523/JNEUROSCI.4284-06.2007.

Shinnar, S., and C. O'Dell.(2004) Febrile Seizures. *Pediatr Ann* 33, no. 6: 394-401. https://doi.org/10.3928/0090-4481-20040601-10.

Smith, G. D., M. J. Gunthorpe, R. E. Kelsell, P. D. Hayes, P. Reilly, P. Facer, J. E. Wright*, et al.*(2002) Trpv3 Is a Temperature-Sensitive Vanilloid Receptor-Like Protein. *Nature* 418, no. 6894: 186-90. https://doi.org/10.1038/nature00894.

Su, W., X. Qiao, W. Wang, S. He, K. Liang, and X. Hong.(2023) Trpv3: Structure, Diseases and Modulators. *Molecules* 28, no. 2. https://doi.org/10.3390/molecules28020774.

Vincent, F., A. Acevedo, M. T. Nguyen, M. Dourado, J. DeFalco, A. Gustafson, P. Spiro*, et al.*(2009) Identification and Characterization of Novel Trpv4 Modulators. *Biochem Biophys Res Commun* 389, no. 3: 490-4. https://doi.org/10.1016/j.bbrc.2009.09.007.

Wang, H., B. Wang, K. P. Normoyle, K. Jackson, K. Spitler, M. F. Sharrock, C. M. Miller*, et al.*(2014) Brain Temperature and Its Fundamental Properties: A Review for Clinical Neuroscientists. *Front Neurosci* 8: 307. https://doi.org/10.3389/fnins.2014.00307.

Xu, H., I. S. Ramsey, S. A. Kotecha, M. M. Moran, J. A. Chong, D. Lawson, P. Ge*, et al.*(2002) Trpv3 Is a Calcium-Permeable Temperature-Sensitive Cation Channel. *Nature* 418, no. 6894: 181-6. https://doi.org/10.1038/nature00882.

Yamashita, T., A. Pala, L. Pedrido, Y. Kremer, E. Welker, and C. C. Petersen.(2013) Membrane Potential Dynamics of Neocortical Projection Neurons Driving Target-Specific Signals. *Neuron* 80, no. 6: 1477-90. https://doi.org/10.1016/j.neuron.2013.10.059.

Zhang, H., X. Sun, H. Qi, Q. Ma, Q. Zhou, W. Wang, and K. Wang.(2019) Pharmacological Inhibition of the Temperature-Sensitive and Ca(2+)-Permeable Transient Receptor Potential Vanilloid Trpv3 Channel by Natural Forsythoside B Attenuates Pruritus and Cytotoxicity of Keratinocytes. *J Pharmacol Exp Ther* 368, no. 1: 21-31. https://doi.org/10.1124/jpet.118.254045.

Figures and Figure Legends

Figure 1: Body Temperature rises to fever levels during regular activity and exposure to higher ambient temperatures.

A. Left: Setup for recording mouse body temperature((T_b) at room temperature using an implanted transponder for non-invasive measurement. Right: Average T_b readings over 6 hours at 5-minute intervals for 10 mice. T_b typically hovers around 37°C during the day.

B. T_b may briefly elevate into fever range (shaded red bars) during regular daily activity. Median with upper and lower limits indicated.

C. T_b readings over 6 hours, at 5-minute intervals for animal 3 in Figure 1B. Shaded red dots indicate time points when T_b enters the fever range.

D. Left: Setup for T_b recordings during infrared light exposure. Right: T_b elevates into the fever range (>38°C) for extended durations, lasting minutes to hours. Average T_b readings over 6 hours at 5-minute intervals for 10 mice.

Figure 2: Spiking in P12-14 cortical excitatory pyramidal neurons remains stable as temperature enters the fever range.

A. Setup for recording L4-evoked postsynaptic potential and spiking in an excitatory pyramidal neuron (PN) at just-subthreshold V_m at 30°C, 36°C and 39°C in mouse primary somatosensory (S1) cortex.
B. Example traces of L4-evoked spikes in L2/3 PN during consecutive recordings at 30°C (black), 36°C (gray), and 39°C (red).
C. Depolarization required to reach spike threshold (ST) in L2/3 PNs during temperature elevations from 30°C to 39°C.
D. Same as (C) for input resistance (R_{in}).
E. Same as (C) for the percentage of spiking L2/3 PNs.
F. Same as in (C) for the spiking distribution.
G. Same as in (C) for the number of spikes.
Each data point represents an individual cell. 37 PNs recorded from 14 animals. Mean with standard error of the mean shown in C, D and G. Statistical significance assessed via one-way repeated measures ANOVA with Tukey's test at α=0.05.

Figure 3: Spiking in P7-8 cortical excitatory pyramidal neurons decreases as temperature enters the fever range.

A. Setup for recording L4-evoked postsynaptic potential and spiking in an excitatory pyramidal neuron (PN) at just-subthreshold V_m at 30°C, 36°C and 39°C in mouse primary somatosensory (S1) cortex.
B. Example traces of L4-evoked spikes in L2/3 PN during consecutive recordings at 30°C (black), 36°C (gray), and 39°C (red).
C. Depolarization required to reach spike threshold (ST) in L2/3 PNs during temperature elevations from 30°C to 39°C.
D. Same as (C) for input resistance (R_{in}).
E. Same as (C) for the percentage of spiking L2/3 PNs.
F. Same as in (C) for the spiking distribution.
G. Same as in (C) for the number of spikes.
Each data point represents an individual cell. 19 PNs recorded from 5 animals. Mean with standard error of the mean shown in C, D and G. Statistical significance assessed via one-way repeated measures ANOVA with Tukey's test at α=0.05.

Figure 4: Increased depolarization at higher spike thresholds helps maintain stable spiking activity in cortical pyramidal neurons during temperature elevations.

A. Illustration demonstrating how temperature-induced changes in spike threshold make spiking more challenging for a neuron, requiring larger levels of depolarization to sustain spiking.
B. Example traces of L4-evoked postsynaptic potentials (PSPs) in L2/3 PN during consecutive recordings at 30°C (black), 36°C (gray), and 39°C (red).
C. Correlation of PSP peak versus spike threshold (ST). r = Pearson correlation coefficient with Deming linear regression.
D. Correlation of input resistance versus ST. r = Pearson correlation coefficient with simple linear regression.
E. Same as D but for input resistance versus PSP.
F. Illustration showing how temperature-induced loss in inhibition (blue IPSP) could lead to larger levels of depolarization. IPSPs typically bring the membrane potential away from the spike threshold.
G. The late PSP peak in L2/3 PNs during temperature elevations from 30°C to 39°C. Statistical significance was evaluated on log-transformed data using one-way repeated measures ANOVA with Tukey's test, with significance at α=0.05.
H. Same as D but for PSP versus Late PSP Peak.
r = Spearman correlation coefficient with simple linear regression.

Figure 5: Cortical neurons that remain active at febrile temperatures spike at higher rates, but the excitatory-inhibitory balance remains unchanged.
A. Setup for *in vivo* recording of spiking in mouse S1 cortex during temperature increases from 36°C to 39°C and cooling back to 36°C.
B. Normalized firing rates from putative excitatory PNs and interneurons obtained from recordings in A.
C. Left: Setup for *ex vivo* recording of L4-evoked postsynaptic potential and spiking in a L2/3 PN at just-subthreshold V_m at 30°C, 36°C and 39°C in mouse S1 cortex. Right: Percent distribution for recorded PNs that never spiked, stopped spiking, stayed spiking, or started spiking during temperature increases from 36°C to 39°C.
D. L2/3 PN spiking activity in neurons that stayed spiking (left), started spiking (middle), and stopped spiking (right) upon temperature increases from 36°C to 39°C.
E. Left: Setup for *ex vivo* recording of L4-evoked excitatory and inhibitory postsynaptic currents (EPSCs and IPSCs, respectively). Right: The excitatory-inhibitory (E-I) balance (defined as E/E+I, the ratio of the EPSC to the total current (EPSC+IPSC) measurements during temperature increases from 36 to 39°C.
F. Activity distribution for *ex vivo* recorded neurons that never spiked, and those that stopped spiking, stayed spiking, or started spiking upon temperature increases from 36°C to 39°C. P-

value = 0.01 indicates a significant increase in the fraction of neurons that stayed spiking during temperature increases from 36°C to 39°C (solid red bar).
In B,D and E, each data point represents an individual cell. Data collected from 5 animals (in B), 11 animals (in C,D), 7 animals (in E) and 9-14 animals (in F). Mean with standard error mean is indicated in B and E. Significance assessed by paired two-tailed t-test (D and E), one-way repeated measures ANOVA with Tukey's test (in B) and binomial test (in F). Significance at α=0.05.

Figure 6: Excitatory pyramidal neurons that remain spiking with temperature elevations into fever range exhibit unique intrinsic properties.
Neurons that spiked at all temperatures (30°C, 36°C, and 39°C) are STAY PNs, while those that stopped spiking at 36°C or 39°C are STOP neurons.
A. Depolarization required to reach spike threshold (ST) in STOP and STAY L2/3 PNs during temperature elevations from 30°C to 39°C.
B. Same as (A) for L4-evoked postsynaptic potentials (PSPs)
C. Correlation of PSP peak versus ST in STAY L2/3 PNs at 30°C, 36°C, and 39°C. r = Pearson correlation coefficient with Deming linear regression.
D. Same as (C) for STOP cells.
E. Same as (A) for the L4-evoked late PSP peak.
F. Same as (A) for spike height.
G. Same as (A) for spike afterhyperpolarization (AHP).
H. Same as (A) for input resistance.
Each data point represents an individual cell in A-H. Data collected from 14 animals. Mean with standard error mean is indicated in A-B and E-H. Significance assessed by one- and two-way repeated measures ANOVA with Tukey's or Sidak post-hoc test, or paired t-test at α=0.05.

Figure 7: Medium spiny neurons (MSNs) that remain spiking with temperature elevations into fever range exhibit unique intrinsic properties.
Neurons that spiked at all temperatures (30°C, 36°C, and 39°C) are STAY MSNs, while those that stopped spiking at 36°C or 39°C are STOP MSNs.
A. Setup for recording evoked spiking in MSNs expressing dopamine (D)1-type receptors (i.e. $D1^+$ MSNs) or D2-type receptors (i.e. $D2^+$ MSNs).
B. Example traces of evoked spikes in $D1^+$ MSN during consecutive recordings at 30°C (black), 36°C (gray), and 39°C (red).
C. Depolarization required to reach spike threshold (ST) in STOP and STAY $D1^+$ MSNs during temperature elevations from 30°C to 39°C.

D. Summed trace (B) for evoked postsynaptic potentials (PSPs).
E. Same as (C) for input resistance.
F. Same as (B) for evoked spikes in $D2^+$ MSNs.
G. Same as (C) for ST in $D2^+$ MSNs.
H. Same as (B) for evoked PSPs in $D2^+$ MSNs.
I. Same as (C) for input resistance in $D2^+$ MSNs
Each data point represents an individual cell in C-D and G and I. Summed trace from all recordings is indicated in D and H. Data collected from 6 animals in C-E and 4 animals in F-G . Mean with standard error mean is indicated in C-D and F-G. Significance assessed by one- and two-way repeated measures ANOVA with Tukey's or Sidak post-hoc test, or paired t-test at $\alpha=0.05$.

Figure 8: Temperature elevations in fever range increase *TRPV3* currents in cortical pyramidal neurons.
A. Setup for recording whole-cell *TRPV3* currents at 30°C (black), 36 °C (grey) and 39°C (red). in cortical excitatory pyramidal neurons (PNs) with bath application of camphor (5mM), a *TPRV3* agonist.
B. Current density-voltage (I-V) relationship of *TRPV3* currents at 30°C (black), 36 °C (grey) and 39°C (red) in WT mice: 11 cells from 4 mice.
C. Scatter dot plots of the current density-voltage measurements.
D. Current density-voltage (I-V) relationship of *TRPV3* currents at 30°C (black) in the presence of camphor (5mM), a *TPRV3* agonist, or camphor (5mM) + *TRPV3* blocker (Forsythoside B, 50 µM) (blue).
E. Same as (**D**) but for 36°C.
F. Same as (**D**) but for 39°C.
G. Current density-voltage (I-V) plot showing the net TRPV3 current (opener – (opener+ blocker) condition).

Figure 9: Inhibiting TRPV3, but not TRPV4 channels, significantly reduced the population of STAY pyramidal neurons and spiking levels at fever temperature.
A. Setup for recording L4-evoked postsynaptic potential and spiking in an excitatory pyramidal neuron (PN) with an intracellular blocker of TRPV3 channels (Forsythoside B, 50 µM) (left) or TRPV4 channels (RN1734, 10 µM) (right) at just-subthreshold V_m at 30°C, 36°C, and 39°C in mouse S1 cortex.
B. Percentages of cell types obtained from experiment in A.

C. Evoked spikes in L2/3 PNs during temperature elevations to 30°C, 36°C, and 39°C with TRPV3 (Forsythoside B, 50 µM) or TRPV4 (RN1734, 10 µM) blockers.

D. Correlation of PSP peak versus spike threshold (ST). r = Pearson correlation coefficient with Deming linear regression.

E. Same as (C) for the L4-evoked late PSP peak.

F. Same as (C) for input resistance.

Each data point represents an individual cell in C, E and F. Data collected from 26 cells in 7 animals for TRPV3 blocker, 24 cells in 6 animals for TRPV4 blocker, and 37 cells from 14 animals for no block condition. Mean with standard error mean is indicated in C, E and F. Significance assessed by one- and two-way repeated measures ANOVA with Tukey's or Sidak post-hoc test at $\alpha=0.05$.